Theory of ultrasonic attenuation at incommensurate phase transitions

A.M. Schorgg* and F. Schwabl
Institut für Theoretische Physik, Physik-Department der Technischen Universität München, James-Franck-Strasse, 85748 Garching, Germany
(Received 29 September 1993)

Acoustic properties below incommensurate phase transitions are severely influenced by phason modes. These unique massless Goldstone modes may lead to coexistence anomalies within the whole phase of broken continuous symmetry. The present theory, based on an order parameter model appropriate for a universality class containing the A_2BX_4 family, employs an extended renormalization scheme. Within this scheme, critical behavior of the Goldstone modes is governed by a fixed point, permitting an exact treatment of the anomalies induced by them. With regard to the coefficient of sound attenuation, the hydrodynamic behavior is not altered by the phason modes, but they lead to a singularity of the scaling function, which describes the crossover from the critical region to the coexistence regime. Determining the universal scaling function and revealing its coexistence anomaly constitute a main result of our study, which explicitly takes fluctuation contributions of the phason and amplitudon modes into account. The sound velocity is predicted to display a minimum in its temperature dependence below the maximum sound attenuation at the same frequency. A treatment of the high-temperature phase is also included. Application to experiments on Rb_2ZnCl_4 and K_2SeO_4 reveals agreement with our theoretical predictions over several orders of magnitude of the scaling variable.

I. INTRODUCTION

We study the influence of Goldstone modes on acoustic anomalies, which occur when a system undergoes a second-order phase transition to a low-temperature phase of broken continuous symmetry. Based on the time-dependent Ginzburg-Landau model, whose renormalization enables an exact treatment of the coexistence anomalies, we determine the coefficient of critical sound attenuation and the sound velocity. Our theory can be applied to the normal-incommensurate phase transition of a large group of materials.

The lattice dynamics of structurally incommensurate phases displays certain aspects that are distinct from ordinary crystalline phases.[1] In the spectrum of dynamical modes associated with the incommensurate modulation, there appear two nondegenerate branches of modes. One of these is known as the amplitudon branch and exhibits common soft-mode behavior, whereas the other, the phason branch, represents the massless Goldstone modes.[2] Since they are massless within the whole low-temperature phase, they may induce new types of anomalies, referred to as coexistence anomalies. A well-known example is the $q^{-\epsilon}$ divergence ($\epsilon = 4 - d$) of the static, wave-number-dependent longitudinal susceptibility at small q.[2,3]

Among other topics, research on materials with incommensurate phases is concerned with the primary dynamical modes and the interactions of these with other degrees of freedom, such as acoustic waves.[4] The presence and form of acoustic anomalies near a phase transition depends on the type of coupling of acoustic and order-parameter modes and gives insight into the underlying lattice dynamics of the structurally incommensurate solid. Our theory is based on a coupling of a single phonon mode to two order-parameter modes, a prototype interaction that has frequently been investigated.[2,5] At this point the interesting question arises as to whether the coupling of the acoustic modes to the phasons leads to an observable effect, thus providing ultrasonic measurements as a tool capable of detecting phasons. For quite some time, the general conclusion has been that the phason has no such effect.[6,7] However, this opinion was based on a Landau-Khalatnikov-type[8] mean-field treatment of the aforementioned coupling. Through the neglect of order-parameter fluctuations, sound attenuation at and above the transition temperature is absent within a mean-field theory. This demonstrates the importance of order-parameter fluctuations, and this is where the phasons come into play. However, because of the peculiarities of phason dynamics at low frequencies, certain subtleties arise. For instance, an erroneous treatment led to the prediction of nonhydrodynamic behavior of the coefficient of sound attenuation,[9] in contradiction to experiment.[10] Even though the importance of anharmonic fluctuation contributions to sound anomalies was emphasized in a more recent paper,[11] the contribution of the Goldstone modes was overestimated and had to be suppressed by the *ad hoc* introduction of an energy gap. While infrared divergent contributions appear at intermediate steps of the perturbation theory, earlier investigations by Dengler and Schwabl showed already that these cancel in the final result, leading to a finite universal amplitude ratio of sound attenuation.[12]

In this paper we use a renormalization scheme appropriate for the specific features of the phason modes. This scheme was introduced by Lawrie[13] for the study of static

coexistence anomalies. Recently its applicability to the dynamical properties was demonstrated by Täuber and Schwabl.[14] A brief account of our theory has been presented in Ref. 15. Besides giving more details and additional results, the range of applicability of our theory is extended to Brillouin scattering experiments.

The velocity and the coefficient of sound attenuation depend on the wave vector $\mathbf{k}$ and frequency of the sound wave ω and on $\tau \propto T - T_I$, where T_I is the transition temperature to the incommensurate phase. We will be able to determine the scaling law for the coefficient of critical attenuation of longitudinal sound modes

$$\alpha(\mathbf{k},\omega,\tau) \propto \omega^2 \mid \tau \mid^{-\rho} g(k\xi,\omega/\omega_{\rm ch}) / A(\mathbf{k},\omega,\mid \tau \mid), \tag{1.1}$$

where the hydrodynamic asymptotics have been separated off $(k = \mid \mathbf{k} \mid)$. This permits the following conclusions: In the hydrodynamic regime, aside from a temperature dependence expressed by a critical exponent ρ, a quadratic frequency dependence is found. Thus the Goldstone modes do not alter the hydrodynamic asymptotics; however, they lead to a cusp singulartity of the scaling function $g(k\xi,\omega/\omega_{\rm ch})$ at small scaling variables $k\xi$ and $\omega/\omega_{\rm ch}$, where ξ is the correlation length and $\omega_{\rm ch}$ is the characteristic order-parameter frequency. This cusp singularity is the unequivocal signature of the Goldstone modes. It already has been predicted by Dengler and one of the present authors.[12] In a recent paper,[16] we obtained the corresponding result by means of a $1/n$ expansion. The present theory puts the prediction of the Goldstone singularity on a firm basis, suitable for a comparison with experiment.

The scaling behavior of the sound velocity is more intricate to analyze, but of course is comprised in our treatment. For fixed frequency, the sound velocity has a minimum at a temperature below the maximum of the attenuation. Application of our theory to Rb_2ZnCl_4 and K_2SeO_4, members of the universality class of our model, leads to good agreement between theoretical predictions and experimental data on sound velocity and attenuation.

This paper is organized as follows: In Sec. II, we present our model free energy including the coupling of the sound wave to the order parameter Φ of the incommensurate phase transition. The dynamics of these modes is described by stochastic equations of motion of the Langevin type. An expression for the coefficient of sound attenuation and the sound velocity is derived by means of a Φ^2 correlation function. In Sec. III we introduce the stochastic functional required for a calculation of the Φ^2 correlation funtion in the low-temperature (incommensurate) phase. Special care is taken with regard to the limiting coexistence behavior, where the Goldstone anomalies show up. The next section is devoted to renormalization of the theory and concludes with an explicit result for the renormalized Φ^2 correlation function. In Sec. V, the renormalization-group equation is integrated by the method of charateristics. The scaling law for the Φ^2 is derived in Sec. VI, and we discuss its implications for the coefficient of sound attenuation and the sound velocity. We determine critical exponents appearing in the asymptotic power laws of the hydrodynamic and critical regimes and the universal crossover scaling functions. In Sec. VII, we give an application of our theory to members of the A_2BX_4 family. In the last section, we summarize our results and discuss further directions of investigation. Appendix A contains a coherent presentation of important properties of the theory within the coexistence limit. Appendix B details the computation of frequency and wave vector integrations necessitated by the fluctuational contributions. In Appendix C we summarize the treatment of the Φ^2 correlation function in the high-temperature phase.

II. ORDER PARAMETER MODEL AND COUPLING TO SOUND WAVES

A. Structurally incommensurate systems

Among the systems that undergo a transition to an incommensurate phase, some substances exhibit a quite complicated scenario with a whole sequence of incommensurate and commensurate phases.[4] In this paper, we focus on the vicinity of the second-order transition at T_I from the high-temperature paraphase to a structurally incommensurate phase extending to T_L, the temperature of the (first) lock-in transition, as shown in Fig. 1. The real-space displacement field corresponding to the one-dimensional incommensurate modulation can be represented by its normal mode coordinates $Q(\mathbf{q})$.[2] We restrict ourselves to systems where the star of soft modes consists of two wave vectors $\pm\mathbf{q}_s$ along one of the principal directions of the Brillouin zone. Within the plane-wave regime, the incommensurate modulation is dominated by the primary Fourier components with wave vectors $\pm\mathbf{q}_s$, i.e., $\langle Q(\mathbf{q})\rangle \propto \delta(\mathbf{q} \pm \mathbf{q}_s)e^{i\varphi_0}$. We therefore use the $Q(\mathbf{q})$ as a primary-order parameter of the normal-to-incommensurate phase transition in the Landau-Ginzburg-Wilson free-energy functional, whose harmonic part is diagonalized by the following transformation

$$\begin{aligned} P_\phi(\mathbf{k}) &= \frac{i}{\sqrt{2}}\left[e^{-i\varphi_0}Q(-\mathbf{q}_s+\mathbf{k}) - e^{i\varphi_0}Q(\mathbf{q}_s+\mathbf{k})\right], \\ P_A(\mathbf{k}) &= \frac{1}{\sqrt{2}}\left[e^{-i\varphi_0}Q(-\mathbf{q}_s+\mathbf{k}) + e^{i\varphi_0}Q(\mathbf{q}_s+\mathbf{k})\right]. \end{aligned} \tag{2.1}$$

The fluctuations of $P_A(\mathbf{k})$ about its finite mean value can be identified with fluctuations of the amplitude of the dis-

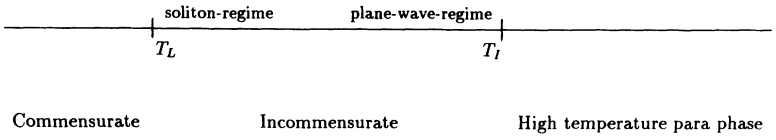

FIG. 1. Sketch of the phase diagram referring to a normal-incommensurate transition at T_I and a lock-in transition at T_L.

placement field.[2] Complementary, $P_\phi(\mathbf{k})$ with vanishing mean value describes fluctuations about the phase $\varphi_\circ$ of the incommensurate displacement field. The dynamical excitations of the order parameter associated with P_ϕ and P_A fluctuations are called phason and amplitudon modes, respectively.

In the following theoretical treatment, for the sake of generality, the two-component order parameter (P_ϕ, P_A) is considered as a special case of an n-component order parameter $\mathbf{\Phi}_\circ$, i.e., $(P_\phi, P_A) \to (\Phi_{\circ 1}, \Phi_{\circ 2})$. By means of the new variables, the effective energy functional within the plane wave regime may be written as[1]

$$\mathcal{H}_\Phi = \frac{1}{2}\sum_{j=1}^{n}\int_{\mathbf{k}}(r_\circ + \mathbf{k}^2)\Phi_{\circ j}(\mathbf{k})\Phi_{\circ j}(-\mathbf{k}) + \frac{\tilde{u}_\circ}{4!}\sum_{i,j=1}^{n}\int_{\mathbf{k}_1}\cdots\int_{\mathbf{k}_4}\Phi_{\circ i}(\mathbf{k}_1)\Phi_{\circ i}(\mathbf{k}_2)\Phi_{\circ j}(\mathbf{k}_3) \times\Phi_{\circ j}(\mathbf{k}_4)\,\delta\Big(\sum_l \mathbf{k}_l\Big)\,, \tag{2.2}$$

which is just the n-component isotropic Heisenberg model. The universality class of the two-component model contains incommensurate solids with orthorhombic D_{2h}^{16} space group of the high-temperature paraphase (e.g., members of the A_2BX_4 family.[17]) As a consequence of the $O(2)$ symmetry of this model, massless Goldstone modes appear in the phase with broken continuous symmetry. In the present case, this is the $P_\phi(\mathbf{k})$ phason mode.

B. Coupling to sound waves

The nature of critical acoustic anomalies crucially depends on the coupling of the sound waves to the order parameter. Here, we investigate a coupling linear in the acoustic phonon variable and bilinear in the primary order parameter[2]

$$\mathcal{H}_{\rm int} = \sum_{\lambda\delta}\int_{\mathbf{k}}\int_{\mathbf{q}_1}\int_{\mathbf{q}_2} U_{\lambda\delta}(\mathbf{q}_1,\mathbf{q}_2)\;\eta_{\lambda\delta}(\mathbf{k})\;Q(\mathbf{q}_1)\,Q(\mathbf{q}_2)\,\delta(\mathbf{k}+\mathbf{q}_1+\mathbf{q}_2)\,. \tag{2.3}$$

The sound wave in (2.3) is described by the components of the strain field $\eta_{\lambda\delta}(\mathbf{k})$. The coupling constants $U_{\lambda\delta}(\mathbf{q}_1,\mathbf{q}_2) = U_{\lambda\delta}(\mathbf{q}_2,\mathbf{q}_1)$ depend on the wave vector of the order-parameter modes involved and obey momentum conservation. Expressing (2.3) in terms of phason and amplitudon modes leads to

$$\mathcal{H}_{\rm int} = \sum_{\lambda\delta}\int_{\mathbf{k}}\int_{\mathbf{q}}\eta_{\lambda\delta}(\mathbf{k})\Big\{\,K_{\lambda\delta}^{(1)}(\mathbf{q},\mathbf{q}+\mathbf{k})\Big[P_\phi(\mathbf{q})P_\phi(-\mathbf{q}-\mathbf{k})+P_A(\mathbf{q})P_A(-\mathbf{q}-\mathbf{k})\Big] +2K_{\lambda\delta}^{(2)}(\mathbf{q},\mathbf{q}+\mathbf{k})\,i\Big[P_\phi(\mathbf{q})P_A(-\mathbf{q}-\mathbf{k})\Big]\Big\}. \tag{2.4}$$

In (2.4), different couplings appear for the quadratic combination $(P_\phi P_\phi + P_A P_A)$ and the mixed bilinear term $(P_\phi P_A)$, respectively

$$K_{\lambda\delta}^{(1)/(2)}(\mathbf{q}_1,\mathbf{q}_2) \equiv \frac{1}{2}\Big[U_{\lambda\delta}(\mathbf{q}_s+\mathbf{q}_1,-\mathbf{q}_s-\mathbf{q}_2) + / - U_{\lambda\delta}(-\mathbf{q}_s+\mathbf{q}_1,\mathbf{q}_s-\mathbf{q}_2)\Big]\,. \tag{2.5}$$

From obvious symmetry properties it follows that $K_{\lambda\delta}^{(1)}(0,0) \neq 0$ is allowed, however $K_{\lambda\delta}^{(2)}(0,0) \equiv 0$. Since the main contribution to integrations in the reciprocal lattice arises from the vicinity of $\pm\mathbf{q}_s$, the couplings are usually expanded, i.e., $U_{\lambda\delta}(\mathbf{q}_s,-\mathbf{q}_s+\mathbf{k}) \sim U_{\lambda\delta} + \sum_\gamma U_{\lambda\delta,\gamma}k^\gamma$. With the help of the expanded coupling functions

$$K_{\lambda\delta}^{(1)}(\mathbf{q}_1,\mathbf{q}_2) \sim U_{\lambda\delta} \tag{2.6}$$

and

$$K_{\lambda\delta}^{(2)}(\mathbf{q}_1,\mathbf{q}_2) \sim \sum_\gamma U_{\lambda\delta,\gamma}(q_1^\gamma + q_2^\gamma)$$

the interaction part reads in terms of the generalized order-parameter fields $\mathbf{\Phi}_\circ$

$$\mathcal{H}_{\rm int} = \sum_{\lambda,\delta}\int_{\mathbf{k}}\eta_{\lambda\delta}(\mathbf{k})\Big[\,U_{\lambda\delta}\;\mathbf{\Phi}_\circ^2(-\mathbf{k}) +2\sum_\gamma U_{\lambda\delta,\gamma}\;\Theta_\circ^\gamma(-\mathbf{k})\Big], \tag{2.7}$$

with the composite fields

$$\mathbf{\Phi}_\circ^2(\mathbf{k}) \equiv \int_{\mathbf{k}_1}\sum_j \Phi_{\circ j}(\mathbf{k}_1)\Phi_{\circ j}(\mathbf{k}-\mathbf{k}_1)\quad, \tag{2.8}$$

$$\Theta_\circ^\gamma(\mathbf{k}) \equiv \int_{\mathbf{k}_1}(2k_1^\gamma - k^\gamma)i\sum_{\alpha=1}^{n-1}\Phi_{\circ\alpha}(\mathbf{k}_1)\Phi_{\circ n}(\mathbf{k}-\mathbf{k}_1). \tag{2.9}$$

Here γ denotes a Cartesian component of both, the external wave vector $\mathbf{k}$ and the internal integration variable $\mathbf{k}_1$. Finally, the components of the deformation are written as a sum of normal coordinates $Q_{\mathbf{k},\kappa}$, i.e., $\eta_{\lambda\delta}(\mathbf{k}) = i\sum_\kappa Q_{\mathbf{k},\kappa}\epsilon_{\mathbf{k},\kappa}^\lambda k^\delta$, with the polarization vector $\boldsymbol{\epsilon}_{\mathbf{k},\kappa}$, polarization κ, and wave vector $\mathbf{k}$. In the total Hamiltonian of the coupled system of phonons and order parameter modes $\mathcal{H} = \mathcal{H}_\Phi + \mathcal{H}_{\rm phon}$, the phonon part $\mathcal{H}_{\rm phon}$ is given by

$$\mathcal{H}_{\text{phon}} = \int_{\mathbf{k}} \sum_{\kappa} \frac{\bar{\rho}}{2} \mid k\, c_{\circ}(\hat{k},\kappa) \mid^2 \mid Q_{\mathbf{k},\kappa} \mid^2 + \int_{\mathbf{k}} \sum_{\kappa} \sum_{\sigma=1}^{4} ik[A_{\sigma}(\hat{k},\kappa)]^{1/2} Q_{\mathbf{k},\kappa}\, \overset{\circ}{\Psi}_{\sigma}(-\mathbf{k}) \,. \tag{2.10}$$

The first term is the purely elastic energy with the mass density $\bar{\rho}$ and the bare sound velocity $c_{\circ}(\hat{k},\kappa)$. The second term describing the interaction is written in a form familiar from the discussion of other structural phase transitions.[18] The order parameter fields $\overset{\circ}{\Psi}_{\sigma}(\mathbf{k})$ and the ensuing coupling coefficients $A_{\sigma}(\hat{k},\kappa)$ are listed in Table I, with the unit wave vector $(\hat{k} = \mathbf{k}/k)$.

Concerning the existence of the coefficients in the expansion of the phonon order-parameter coupling, one has to specify the space group of the normal phase of the incommensurate solid. In this work we consider systems with K_2SeO_4 structure, i.e., D_{2h}^{16} space group. In that case the zeroth-order coefficients $U_{\lambda\delta}$ are nonvanishing for the diagonal elements $(\lambda = \delta)$ only. Of the first order coefficients $U_{\lambda\delta,\gamma}$ the nonvanishing ones are listed in Refs. 5 and 19. The explicit form of the coupling coefficients $A_{\sigma}(\hat{k},\kappa)$ for the K_2SeO_4 structure is given in Table II. From this table the couplings possible for acoustic modes propagating along high-symmetry directions can be easily read off. Thus for longitudinal sound modes coupling of the type $\sigma = 1,2$ is allowed and for transverse sound modes that with $\sigma = 3,4$.

C. Phonon dispersion relation

With reference to the linear wave vector dependence, the phason is sometimes called an acousticlike mode. However, acoustic phonons have a damping proportional to k^2, and are always underdamped at small k. For phasons, the damping is finite at $k = 0$, and therefore they are always overdamped for small k,[20] as described in the following Langevin-type equation of motion[21]

$$\dot{\Phi}_{\circ j}(\mathbf{k},t) = -\lambda_{\circ} \frac{\delta\mathcal{H}}{\delta\Phi_{\circ j}(-\mathbf{k},t)} + r_j(\mathbf{k},t) \,, \qquad j = (1,\ldots,n) \tag{2.11}$$

with

$$\langle r_j(\mathbf{k},t)\rangle = 0 \,,$$

$$\langle r_i(\mathbf{k},t) r_j(\mathbf{k}',t')\rangle = 2\lambda_{\circ}\delta_{i,j}\delta(\mathbf{k}-\mathbf{k}')\delta(t-t') \,.$$

TABLE I. Coupling coefficients and order-parameter fields appearing in the interaction of acoustic modes with the order parameter near incommensurate phase transitions. $(\gamma_2 = x,\ \gamma_3 = y,\ \gamma_4 = z)$.

σ	$\left(A_{\sigma}(\hat{k},\kappa)\right)^{1/2}$	$\circ\Psi_{\sigma}(\mathbf{k})$
1	$\frac{1}{k}\sum_{\lambda,\delta} \epsilon^{\lambda}_{\mathbf{k},\kappa} k^{\delta} U_{\lambda\delta}$	$\Phi^2_{\circ}(\mathbf{k})$
2,3,4	$\frac{1}{k}\sum_{\lambda,\delta} \epsilon^{\lambda}_{\mathbf{k},\kappa} k^{\delta} U_{\lambda\delta,\gamma_\sigma}$	$2\Theta^{\gamma_\sigma}_{\circ}(\mathbf{k})$

TABLE II. Explicit form of the coupling coefficients for K_2SeO_4 structure $(\mathbf{q}_s \parallel \mathbf{a}^*)$.

σ	$\left(A_{\sigma}(\hat{k},\kappa)\right)^{1/2}$
1	$\frac{1}{k}\sum_{\lambda} \epsilon^{\lambda}_{\mathbf{k},\kappa} k^{\lambda} U_{\lambda\lambda}$
2	$\frac{1}{k}\sum_{\lambda} \epsilon^{\lambda}_{\mathbf{k},\kappa} k^{\lambda} U_{\lambda\lambda,x}$
3	$\frac{1}{k}\left(\epsilon^{y}_{\mathbf{k},\kappa} k^{x} U_{yx,y} + \epsilon^{x}_{\mathbf{k},\kappa} k^{y} U_{xy,y}\right)$
4	$\frac{1}{k}\left(\epsilon^{x}_{\mathbf{k},\kappa} k^{z} U_{xz,z} + \epsilon^{z}_{\mathbf{k},\kappa} k^{x} U_{zx,z}\right)$

The equation of motion for the acoustic mode reads

$$\bar{\rho}\,\ddot{Q}_{\mathbf{k},\kappa}(t) = -\frac{\delta\mathcal{H}}{\delta Q_{-\mathbf{k},\kappa}(t)} - \bar{\rho}\, D_{\kappa} k^2\, \dot{Q}_{\mathbf{k},\kappa}(t) + R_{\kappa}(\mathbf{k},t) \,, \tag{2.12}$$

with

$$\langle R_{\kappa}(\mathbf{k},t)\rangle = 0 \,,$$

$$\langle R_{\kappa}(\mathbf{k},t) R_{\kappa'}(\mathbf{k}',t')\rangle = 2\bar{\rho} D_{\kappa}\mathbf{k}^2 \delta_{\kappa,\kappa'}\delta(\mathbf{k}-\mathbf{k}')\delta(t-t') \,,$$

where D_{κ} is the bare damping. The stochastic forces $r_j(\mathbf{k},t)$ of (2.11) and $R_{\kappa}(\mathbf{k},t)$ of (2.12) produce a Gaussian white noise obeying the Einstein relations.

An investigation of critical behavior of sound modes requires the interacting phonon propagator. Recently, a treatment of this problem has been elaborated for a generalized class of dynamic models by Drossel and one of the present authors.[22] As a result, the phonon dispersion relation for the above model can be written in the following way

$$\omega^2 + D(\hat{k},\omega,\kappa)k^2 i\omega - c^2(\hat{k},\omega,\kappa)k^2 = 0 \quad , \tag{2.13}$$

with the interacting damping $D(\hat{k},\omega,\kappa)$ and sound velocity $c(\hat{k},\omega,\kappa)$, which are shifted from their bare values through the appearance of phonon self-energy contributions. In this paper our main interest will be directed towards the description of longitudinal sound modes propagating along high-symmetry directions, i.e., $\hat{k} \to \mathbf{e}_i, \kappa \to l$. Inspection of Table II then yields two self-energy contributions for longitudinal phonons, steming from the isotropic coupling due to A_1 and the anisotropic coupling due to A_2. However, in the low-frequency regime accessible to ultrasonic experiments, the anisotropic coupling yields only a negligible contribution to the acoustic anomalies[11] compared to the isotropic coupling, and for that reason, we omit it from our theoretical expressions. For transverse sound modes, anisotropic coupling (see A_3 and A_4 in Table II) represents the interaction involving the lowest number of coupled modes, and a summary of the properties of its contribution to sound anomalies will be given at the end of Sec. VI.

Here, we proceed with the treatment of isotropic coupling, yielding the following expressions for the damping and sound velocity

$$D(\hat{k},\omega,\kappa) = D_{\kappa} - \frac{c^2_{\circ}(\hat{k},\kappa)}{\omega}\, \text{Im}\, \frac{1}{1 + 4n(\gamma_i)^2\ \overset{\circ}{\Pi}(\mathbf{k},\omega)} \,, \tag{2.14}$$

$$c^2(\hat{k},\omega,\kappa) = c_\circ^2(\hat{k},\kappa)\ \mathrm{Re}\ \frac{1}{1+4n(\gamma_i)^2\ \overset{\circ}{\Pi}(\mathbf{k},\omega)}\ , \qquad (2.15)$$

where the $\mathbf{\Phi}^2$ correlation function is an expectation value of composite order-parameter fields

$$2n\ \overset{\circ}{\Pi}(\mathbf{k},\omega) = -\frac{1}{2}\int_0^\infty dt\, e^{i\omega t}\ \frac{d}{dt}\ \langle \mathbf{\Phi}_\circ^2(\mathbf{k},t)\ \mathbf{\Phi}_\circ^2(-\mathbf{k},0)\rangle, \qquad (2.16)$$

and $(\gamma_i)^2 = A_1(\mathbf{e}_i,l)/[\bar{\rho}c_\circ^2(\mathbf{e}_i,l)]$ is an abbreviation for the coupling strength. The index i is determined by the direction along which the acoustic phonon propagates.

In the computation of the $\mathbf{\Phi}^2$ correlation function, the phonon degrees of freedom contained in (2.10) can be integrated out. Concerning statics, this can be achieved by completing the square, yielding a Gaussian integral for the acoustic degrees of freedom

$$\mathcal{H}_{\mathrm{phon}} = \int_{\mathbf{k}}\sum_{\kappa}\Big\{\ \frac{\bar{\rho}}{2}\mid k\,c_\circ(\hat{k},\kappa)\mid^2\mid \bar{Q}_{\mathbf{k},\kappa}\mid^2 + \frac{1}{2\bar{\rho}}\frac{1}{\mid c_\circ(\hat{k},\kappa)\mid^2}\Big[\sum_{\sigma=1}^{4}[A_\sigma(-\hat{k},\kappa)]^{1/2}\ \overset{\circ}{\Psi}_\sigma\ (\mathbf{k})\Big]$$
$$\times\Big[\sum_{\sigma'=1}^{4}[A_{\sigma'}(\hat{k},\kappa)]^{1/2}\ \overset{\circ}{\Psi}_{\sigma'}\ (-\mathbf{k})\Big]\Big\}\ , \qquad (2.17)$$

with shifted normal coordinates

$$\bar{Q}_{\mathbf{k},\kappa} = Q_{\mathbf{k},\kappa} + \sum_{\sigma=1}^{4}\frac{ik[A_\sigma(-\hat{k},\kappa)]^{1/2}}{\bar{\rho}\mid kc_\circ(\hat{k},\kappa)\mid^2}\ \overset{\circ}{\Psi}_\sigma\ (\mathbf{k})\quad . \qquad (2.18)$$

Obviously, elimination of the phonons introduces vertices of the order parameter fields not contained in the initial Hamiltonian. Out of the second term contained in (2.17), there is a contribution similar to the well-known $\mathbf{\Phi}_\circ^4$ vertex, isotropic in order parameter space, but whose prefactor depends on direction in wave-vector space in case of elastic anisotropy. For an elastically isotropic system, the only effect of the acoustic phonons thus would be a shift of the quartic coupling constant $\tilde{u}_\circ \rightarrow u_\circ$ from Eq. (2.2).[22] For an elastically anisotropic system, the significance of this kind of vertex has been investigated in a quite general context, revealing the importance of the sign of the specific-heat exponent α.[23] As a conclusion it follows that for negative α, which is the case for the systems under consideration ($n = 2$, $d = 3$), the critical behavior including the phonon coupling is unchanged with respect to the rigid system. Since the bare value of the quartic coupling constant is unknown and substituted in later applications of the theory by its corresponding universal fixed point value, we neglect this vertex in the present situation. Concerning the continuous symmetry of our model, one has to be aware that the additional terms in (2.17) are not rotationally invariant. However, the extra wave number dependence of the composite order-parameter fields denoted explicitly in Eq. (2.9) renders these vertices irrelevant.

Finally we turn to the dynamic aspects of the phonon order-parameter coupling. Since the dynamics of the sound mode is fast compared to the order-parameter dynamics, the bare sound velocity and damping are irrelevant quantities for the computation of expectation values.[22] The $\mathbf{\Phi}^2$ correlation function does not actually involve the complete energy functional $\mathcal{H}$, but only the part $\mathcal{H}_{\mathbf{\Phi}}$. Thus it is a quantity of pure critical dynamics. Equation (2.14) is closely related to, but not identical with, an earlier phenomenological approach,[24] which is confirmed in significant limiting cases.

In ultrasonics, one uses the coefficient of sound attenuation $\alpha(\mathbf{k},\omega,\kappa)$, which is related to the damping $D(\hat{k},\omega,\kappa)$ via

$$\alpha(\mathbf{k},\omega,\kappa) = \frac{\omega^2}{2c^3(\hat{k},\omega,\kappa)}\ D(\hat{k},\omega,\kappa)\quad . \qquad (2.19)$$

Through the appearance of $\hat{k}$, we express the dependence on the direction of the sound wave, whose frequency and wave numbers are related through (2.15).

III. LOW-TEMPERATURE PHASE AND COEXISTENCE BEHAVIOR

A. Dynamical functional

In the phase of broken symmetry, the expectation value of the order parameter is nonzero, and without loss of generality we assume orientation along the n axis

$$\langle\Phi_{\circ i}\rangle = \sqrt{\frac{3}{u_\circ}}\ m_\circ\ \delta_{n,i}\quad . \qquad (3.1)$$

It will be convenient to introduce new fields

$$\mathbf{\Phi}_\circ(\mathbf{k},\omega) \rightarrow \begin{pmatrix} \pi_\circ^\alpha(\mathbf{k},\omega) \\ \sqrt{\frac{3}{u_\circ}}m_\circ\delta(\mathbf{k})\delta(\omega) + \sigma_\circ(\mathbf{k},\omega)\end{pmatrix}$$
$$(\alpha = 1,\ldots,n-1)\ , \qquad (3.2)$$

where the longitudinal field $\sigma_\circ(\mathbf{k},\omega)$ has zero expectation value and the $(n-1)$ transverse fields $\boldsymbol{\pi}_\circ(\mathbf{k},\omega) = (\pi_\circ^1(\mathbf{k},\omega),\ldots,\pi_\circ^{n-1}(\mathbf{k},\omega))$ are massless due to a Ward identity.[14] From $\langle\sigma_\circ(0,0)\rangle = 0$, a relation between the temperature variable $r_\circ$ and $m_\circ$ can be derived: $r_\circ + \frac{m_\circ^2}{2} = A$. The quantity A is determined perturbatively and will give rise to counterterms appearing in the perturbation theory when the temperature dependence in our model is parametrized by $m_\circ$ instead of $r_\circ$.[14]

The model for the critical dynamics contained in Eq. (2.11) can be equivalently represented by the stochastic functional $\mathcal{J}$ in a path integral formulation.[25,26] Introduction of auxiliary fields $\tilde{\mathbf{\Phi}}_\circ = (\tilde{\pi}_\circ^1,\ldots,\tilde{\pi}_\circ^{n-1},\tilde{\sigma}_\circ)$ reduces the complexity of the stochastic functional,[27] which can be split into a harmonic part $\mathcal{J}_{\mathrm{harm}}$ and an interaction part $\mathcal{J}_{\mathrm{int}}$. To facilitate giving explicit expressions, we introduce the shorthand notation

$$\int_{\mathbf{k}_1,\ldots,\mathbf{k}_p}\int_{\omega_1,\ldots,\omega_p} \Psi^{i_1} * \cdots * \Psi^{i_p}$$
$$= \int \frac{d^d\mathbf{k}_1}{(2\pi)^d}\cdots\int \frac{d^d\mathbf{k}_p}{(2\pi)^d}\int\frac{d\omega_1}{2\pi}\cdots\int\frac{d\omega_p}{2\pi}\Psi^{i_1}(\mathbf{k}_1,\omega_1)\cdots\Psi^{i_p}(\mathbf{k}_p,\omega_p)\delta\left(\sum_{l=1}^{p}\mathbf{k}_l\right)\delta\left(\sum_{l=1}^{p}\omega_l\right), \quad (3.3)$$

where the Ψ^i in (3.3) stand for any of the fields $\pi_\circ^\alpha$, $\sigma_\circ$, $\tilde{\pi}_\circ^\alpha$, or $\tilde{\sigma}_\circ$. The harmonic part of the dynamic functional in the phase of broken symmetry clearly distinguishes between transverse and longitudinal modes:

$$\mathcal{J}_{\text{harm}}[\{\pi_\circ^\alpha\},\sigma_\circ,\{\tilde{\pi}_\circ^\alpha\},\tilde{\sigma}_\circ] = \int_{\mathbf{k}_1,\mathbf{k}_2}\int_{\omega_1,\omega_2}\Bigg[\sum_\alpha \lambda_\circ\,\tilde{\pi}_\circ^\alpha\tilde{\pi}_\circ^\alpha + \lambda_\circ\,\tilde{\sigma}_\circ\tilde{\sigma}_\circ - \sum_\alpha\tilde{\pi}_\circ^\alpha\left[i\omega_1+\lambda_\circ k_1^2\right]\pi_\circ^\alpha$$
$$-\tilde{\sigma}_\circ\left[i\omega_1+\lambda_\circ(m_\circ^2+k_1^2)\right]\sigma_\circ\Bigg]. \quad (3.4)$$

From $\mathcal{J}_{\text{harm}}$, the harmonic propagators are given by

$$\langle\pi_\circ^\alpha(\mathbf{k},\omega)\tilde{\pi}_\circ^\beta(\mathbf{q},\tilde{\omega})\rangle_{\text{harm}} = \delta(\mathbf{k}+\mathbf{q})\,\delta(\omega+\tilde{\omega})\,\delta_{\alpha,\beta}\quad\frac{1}{\lambda_\circ k^2 - i\omega}\quad, \quad (3.5)$$

$$\langle\sigma_\circ(\mathbf{k},\omega)\tilde{\sigma}_\circ(\mathbf{q},\tilde{\omega})\rangle_{\text{harm}} = \delta(\mathbf{k}+\mathbf{q})\,\delta(\omega+\tilde{\omega})\quad\frac{1}{\lambda_\circ(m_\circ^2+k^2)-i\omega}. \quad (3.6)$$

The interaction part contains vertices with four fluctuating fields, and as a new feature of the low-temperature phase there are vertices with three fluctuating fields

$$\mathcal{J}_{\text{int}}[\{\pi_\circ^\alpha\},\sigma_\circ,\{\tilde{\pi}_\circ^\alpha\},\tilde{\sigma}_\circ] = -\lambda_\circ\frac{\sqrt{3u_\circ}}{6}m_\circ\int_{\mathbf{k}_1,\mathbf{k}_2,\mathbf{k}_3}\int_{\omega_1,\omega_2,\omega_3}\Big[\sum_\alpha 2\tilde{\pi}_\circ^\alpha\pi_\circ^\alpha\sigma_\circ + \sum_\alpha\tilde{\sigma}_\circ\pi_\circ^\alpha\pi_\circ^\alpha + 3\tilde{\sigma}_\circ\sigma_\circ\sigma_\circ\Big]$$
$$-\frac{\lambda_\circ u_\circ}{6}\int_{\mathbf{k}_1,\ldots,\mathbf{k}_4}\int_{\omega_1,\ldots,\omega_4}\Big[\sum_{\alpha,\beta}\tilde{\pi}_\circ^\alpha\pi_\circ^\alpha\pi_\circ^\beta\pi_\circ^\beta + \sum_\alpha\tilde{\pi}_\circ^\alpha\pi_\circ^\alpha\sigma_\circ\sigma_\circ + \sum_\alpha\tilde{\sigma}_\circ\sigma_\circ\pi_\circ^\alpha\pi_\circ^\alpha + \tilde{\sigma}_\circ\sigma_\circ\sigma_\circ\sigma_\circ\Big]. \quad (3.7)$$

We remark that the contribution of a Jacobian $\mathcal{J}_{FD}[\Phi_\circ,\tilde{\Phi}_\circ] = \int d^d\mathbf{x}\int dt\;\frac{\lambda_\circ}{2}\frac{\delta}{\delta\Phi_{\circ j}}\frac{\delta\mathcal{H}_\Phi}{\delta\tilde{\Phi}_{\circ j}}$ guarantees the cancellation of acausal terms in perturbation theory. Because the temperature is parametrized in terms of $m_\circ$ instead of $r_\circ$ in our theory, an additional counterterm,

$$\mathcal{J}_{\text{count}} = -A\int_{\mathbf{k}_1,\mathbf{k}_2}\int_{\omega_1,\omega_2}\Big[\sum_\alpha\lambda_\circ\tilde{\pi}_\circ^\alpha\pi_\circ^\alpha + \lambda_\circ\tilde{\sigma}_\circ\sigma_\circ\Big] - \lambda_\circ\sqrt{3/u_\circ}m_\circ A\tilde{\sigma}_\circ(0,0)\,,$$

appears, which is depicted by the symbol $\times$ in the following diagrammatic representation of perturbation theory.

B. The Φ^2–correlation function

Our goal is the computation of the Φ^2–correlation function (2.16). With the help of a fluctuation-dissipation theorem,[26] it is expressed as a composite field response function

$$\frac{2n}{\lambda_\circ}\;\overset{\circ}{\Pi}(\mathbf{k},\omega) = \langle\Phi_\circ^2(\mathbf{k},\omega)\,(\Phi_\circ\tilde{\Phi}_\circ)(-\mathbf{k},-\omega)\rangle\,. \quad (3.8)$$

We introduce cumulants using the notation

$$\overset{\circ}{G}{}^{(\tilde{M},M)}_{(\tilde{N},N)}(\mathbf{k}_1,\omega_1;\ldots;\mathbf{k}_{\tilde{M}},\omega_{\tilde{M}};\ldots;\mathbf{k}_M,\omega_M;\ldots;\mathbf{k}_{\tilde{N}},\omega_{\tilde{N}};\ldots;\mathbf{k}_N,\omega_N)\quad, \quad (3.9)$$

where the index $\tilde{M}$ specifies the number of $(\boldsymbol{\pi}_\circ\tilde{\boldsymbol{\pi}}_\circ+\sigma_\circ\tilde{\sigma}_\circ)(\mathbf{k},\omega)$ insertions, M that of $(\boldsymbol{\pi}_\circ^2+\sigma_\circ^2)(\mathbf{k},\omega)$ insertions and $\tilde{N},N$ counts external fields $\tilde{\sigma}_\circ,\sigma_\circ$, respectively; $(\boldsymbol{\pi}_\circ^2+\sigma_\circ^2)(\mathbf{k},\omega)$ is a short-hand notation for the wave-vector- and frequency-dependent composite operator

$$(\boldsymbol{\pi}_\circ^2+\sigma_\circ^2)(\mathbf{k},\omega)\;\equiv\;\int_{\mathbf{k}_1}\int_{\omega_1}\left(\sum_{\alpha=1}^{n-1}\pi_\circ^\alpha(-\mathbf{k}_1,-\omega_1)\pi_\circ^\alpha(\mathbf{k}+\mathbf{k}_1,\omega+\omega_1)+\sigma_\circ(-\mathbf{k}_1,-\omega_1)\sigma_\circ(\mathbf{k}+\mathbf{k}_1,\omega+\omega_1)\right), \quad (3.10)$$

and $(\boldsymbol{\pi}_\circ\tilde{\boldsymbol{\pi}}_\circ+\sigma_\circ\tilde{\sigma}_\circ)(\mathbf{k},\omega)$ is defined analogously. The Φ^2 correlation function is now expressed as a sum of cumulants

$$\frac{2n}{\lambda_\circ}\;\overset{\circ}{\Pi}(\mathbf{k},\omega)\;=\overset{\circ}{G}{}^{(1,1)}_{(0,0)}(\mathbf{k},\omega)+\sqrt{\frac{3}{u_\circ}}m_\circ\;\overset{\circ}{G}{}^{(0,1)}_{(1,0)}(-\mathbf{k},-\omega)+2\sqrt{\frac{3}{u_\circ}}m_\circ\;\overset{\circ}{G}{}^{(1,0)}_{(0,1)}(\mathbf{k},\omega)+\frac{6}{u_\circ}m_\circ^2\;\overset{\circ}{G}{}^{(0,0)}_{(1,1)}(\mathbf{k},\omega)\,. \quad (3.11)$$

In our notation for the arguments of the cumulants in (3.11) it is sufficient to display explicitly only the wave vector and the frequency belonging to the last nonzero index, according to the sequence of (3.9).

In preparation of the next section, we wish to relate the cumulants of (3.11) to vertex functions. As usual, this is achieved by a Legendre transformation, and the lowest ones are

$$\overset{\circ}{\Gamma}{}^{(0,0)}_{(1,1)}(\mathbf{k},\omega) = \frac{1}{\overset{\circ}{G}{}^{(0,0)}_{(1,1)}(-\mathbf{k},-\omega)}, \tag{3.12}$$

$$\overset{\circ}{\Gamma}{}^{(1,0)}_{(1,0)}(\mathbf{k},\omega) = -\sqrt{\frac{3}{u_\circ}}m_\circ - \frac{\overset{\circ}{G}{}^{(1,0)}_{(0,1)}(\mathbf{k},\omega)}{\overset{\circ}{G}{}^{(0,0)}_{(1,1)}(\mathbf{k},\omega)}, \tag{3.13}$$

$$\overset{\circ}{\Gamma}{}^{(0,1)}_{(0,1)}(\mathbf{k},\omega) = -2\sqrt{\frac{3}{u_\circ}}m_\circ - \frac{\overset{\circ}{G}{}^{(0,1)}_{(1,0)}(\mathbf{k},\omega)}{\overset{\circ}{G}{}^{(0,0)}_{(1,1)}(-\mathbf{k},-\omega)}, \tag{3.14}$$

$$\overset{\circ}{\Gamma}{}^{(1,1)}_{(0,0)}(\mathbf{k},\omega) = -\overset{\circ}{G}{}^{(1,1)}_{(0,0)}(\mathbf{k},\omega) + \frac{\overset{\circ}{G}{}^{(1,0)}_{(0,1)}(\mathbf{k},\omega)\,\overset{\circ}{G}{}^{(0,1)}_{(1,0)}(-\mathbf{k},-\omega)}{\overset{\circ}{G}{}^{(0,0)}_{(1,1)}(\mathbf{k},\omega)}. \tag{3.15}$$

With these vertex functions, the $\mathbf{\Phi}^2$−correlation function (3.11) can be expressed by

$$\frac{2n}{\lambda_\circ}\overset{\circ}{\Pi}(\mathbf{k},\omega) = -\overset{\circ}{\Gamma}{}^{(1,1)}_{(0,0)}(\mathbf{k},\omega) + \frac{\overset{\circ}{\Gamma}{}^{(1,0)}_{(1,0)}(\mathbf{k},\omega)\,\overset{\circ}{\Gamma}{}^{(0,1)}_{(0,1)}(-\mathbf{k},-\omega)}{\overset{\circ}{\Gamma}{}^{(0,0)}_{(1,1)}(-\mathbf{k},-\omega)}. \tag{3.16}$$

In the computation of the expectation values contained in the cumulants of (3.11), the explicit form of $\mathcal{J}_{\text{harm}}$ and $\mathcal{J}_{\text{int}}$ leads to the diagrams of Fig. 2 in one-loop order. Before going into further computational details, important conclusions can be drawn with respect to the limiting coexistence behavior.

C. Coexistence limit

At the transition temperature $T = T_I$, the order parameter has zero expectation value ($m_\circ = 0$), and critical phenomena arise from n fluctuating critical modes. At any temperature below the transition point, with no external field applied, we are confronted with a continuously broken symmetry. There are $(n-1)$ massless Goldstone modes and one massive longitudinal mode, leading to different low-frequency and low-wave-number behavior of these modes. This is readily demonstrated by the harmonic response functions (3.5) and (3.6) in a heuristic way: For fixed $T < T_I$ ($m_\circ$ finite), the longitudinal response function attains a finite value as frequency and the wave number tends to zero. However, the transverse functions exhibit a divergence in this limit. The distinct behavior of longitudinal and transverse modes in the coexistence limit $(\mathbf{k},\omega \to 0)$, can also be simulated through

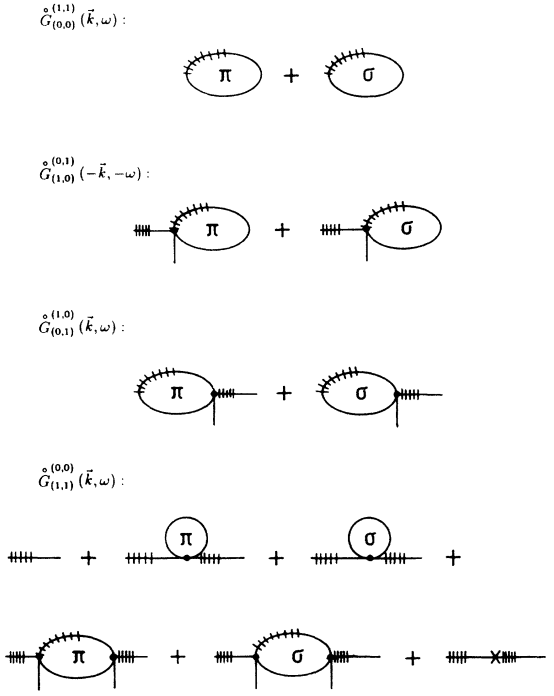

FIG. 2. One-loop diagrams for the cumulants contributing to the $\mathbf{\Phi}^2$ correlation function.

an artificial limit, where the mass is taken to infinity ($m_\circ^2 \to \infty$) at finite $\mathbf{k}$ and ω. The procedure has been discussed in detail for static[13] as well as time-dependent models.[14] Deferring the details to Appendix A, we mention that after a nonlinear transformation of the fields $\tilde{\boldsymbol{\pi}}_\circ, \tilde{\sigma}_\circ, \boldsymbol{\pi}_\circ, \sigma_\circ$ the dynamic functional in the coexistence limit $\mathcal{J}|_{CL}$ becomes a Gaussian theory, permitting an exact solution. Because the transformation is nonlinear, the exact treatment of the cumulants amounts to a nontrivial loop order with respect to the fields $\tilde{\boldsymbol{\pi}}_\circ, \tilde{\sigma}_\circ, \boldsymbol{\pi}_\circ, \sigma_\circ$. Even though our later treatment will be perturbative, it includes an exact limit.

We illustrate this by considering the $\mathbf{\Phi}^2$ correlation function. For the limiting model, the cumulants of (3.11) can be obtained exactly (see Appendix A) yielding

$$2n\,\overset{\circ}{\Pi}(\mathbf{k},\omega)\Big|_{CL} = \frac{6}{u_\circ}. \tag{3.17}$$

We would like to remark that the expectation value $\langle \boldsymbol{\pi}_\circ^2\,(\boldsymbol{\pi}_\circ\tilde{\boldsymbol{\pi}}_\circ)\rangle\big|_{CL}$ given by the infrared divergent transverse bubble (Appendix B), which appears at intermediate steps (Appendix A), has dropped out due to a nonobvious cancellation. This nontrivial observation has been also made in the treatment within the spherical model.[16]

IV. RENORMALIZATION OF CRITICAL AND GOLDSTONE SINGULARITIES

A. Renormalization scheme

The critical behavior in a field theoretical formulation can be obtained by use of the minimal subtraction

procedure,[28,29] where renormalization is carried out in such a way that after the cutoff in momentum space is sent to infinity, the renormalized theory is free of poles at $\varepsilon = 0$, where $\varepsilon = 4 - d$ and d is the number of spatial dimensions. These poles are removed by means of Z factors just designed for this purpose. In the framework of minimal subtraction, the Z factors contain only the poles but no contributions that are finite in the limit $\epsilon \to 0$.

In the phase of broken symmetry, transverse and longitudinal modes are different in that the first ones have a divergent correlation length along the whole coexistence line, while the longitudinal fluctuations freeze out as the mass parameter of the theory is taken to infinity. The ε-pole structure of the theory might be affected too, which can be taken into account, by allowing the renormalization scheme to be extended by temperature-dependent contributions. Such a scheme was proposed by Lawrie for an investigation of Goldstone anomalies in the context of statics.[13] The renormalization prescription is analogous to that introduced by Amit and Goldschmidt[30] for the study of crossover phenomena at bicritical points. Another variant of this renormalization scheme was used for a field theoretical description for the static crossover in dipolar ferromagnets.[31] Recently, Lawries ideas were adapted to the study of coexistence behavior within time-dependent models by Täuber and Schwabl.[14]

In terms of vertex functions, the renormalization scheme is characterized by two requirements: Firstly, the renormalized vertex functions contain no poles at $\varepsilon = 0$. Secondly, after extraction of an overall power of the renormalized temperature variable m, the vertex functions remain finite in the limit $m \to \infty$ at fixed, nonzero wave vector and frequency. This has to be satisfied order by order in an expansion in powers of the renormalized coupling constant.

The Z factors for the renormalization of the temperature variable, the coupling constant and the relaxation rate are introduced as follows:

$$m^2 = Z_m^{-1} m_\circ^2 \mu^{-2}, \quad u = Z_u^{-1} A_d \mu^{-\epsilon} u_\circ, \quad \lambda = Z_\lambda^{-1} \lambda_\circ \, . \tag{4.1}$$

The index $\circ$ serves to distinguish the unrenormalized quantities, which have been used up to now, from the renormalized ones, without label. A wave-number scale μ renders renormalized quantities dimensionless, and A_d is a geometric constant (Appendix B). Through field renormalization

$$\begin{aligned} \pi^\alpha &= Z_\pi^{1/2} \pi_\circ^\alpha, \quad \sigma = Z_\sigma^{1/2} \sigma_\circ \, , \\ \tilde{\pi}^\alpha &= Z_{\tilde{\pi}}^{1/2} \tilde{\pi}_\circ^\alpha, \quad \tilde{\sigma} = Z_{\tilde{\sigma}}^{1/2} \tilde{\sigma}_\circ \, , \end{aligned} \tag{4.2}$$

the renormalized vertex functions are related to their unrenormalized counterparts by

$$\Gamma^{(\tilde{M},M)}_{(\tilde{N},N)} = Z_{\Phi\tilde{\Phi}}{}^{\tilde{M}} \, Z_{\Phi^2}{}^{M} (Z_{\tilde{\sigma}})^{-\tilde{N}/2} (Z_\sigma)^{-N/2} \, \overset{\circ}{\Gamma}{}^{(\tilde{M},M)}_{(\tilde{N},N)} - A^{(\tilde{M},M)}_{(\tilde{N},N)} \, , \tag{4.3}$$

with

$$A^{(\tilde{M},M)}_{(\tilde{N},N)} = \delta_{1,\tilde{M}} \delta_{1,M} \delta_{0,\tilde{N}} \delta_{0,N} \times \left[Z_{\Phi\tilde{\Phi}} \, Z_{\Phi^2} \, Re \left\{ \overset{\circ}{\Gamma}{}^{(\tilde{M},M)}_{(\tilde{N},N)} \right\} \right]_{\text{sing}} \, . \tag{4.4}$$

Hereby, composite order-parameter fields are multiplicatively renormalizable,[13] requiring two more Z factors $Z_{\Phi\tilde{\Phi}}$ and Z_{Φ^2}. The real part Re $\{\overset{\circ}{\Gamma}{}^{(1,1)}_{(0,0)}\}$ requires the additional subtractive renormalization (4.4), which is only a technical point.

Because of Ward identities and other relations, the above Z factors are not independent.[14] The definition (3.1) of the order-parameter expectation value yields $Z_u = Z_m Z_\sigma$ and the composite fields $\mathbf{\Phi}_\circ \mathbf{\Phi}_\circ$ and $(\mathbf{\Phi}_\circ \lambda_\circ \tilde{\mathbf{\Phi}}_\circ)$ are renormalized by the same Z factor, as well as $Z_\pi^{1/2} = Z_{\tilde{\pi}}^{1/2} Z_\lambda^{-1}$ and $Z_\sigma^{1/2} = Z_{\tilde{\sigma}}^{1/2} Z_\lambda^{-1}$.

B. Renormalization in perturbation theory

In one-loop order, there is no field renormalization, nor does the kinetic coefficient renormalize[14] $Z_\pi = Z_{\tilde{\pi}} = Z_\sigma = Z_{\tilde{\sigma}} = Z_\lambda = 1$. Within model A, we are left only with the following Z factors

$$\begin{aligned} Z_u(u_\circ, m_\circ^2) &= Z_m(u_\circ, m_\circ^2) \\ &= 1 + \frac{n-1}{6\varepsilon} u_\circ A_d \mu^{-\varepsilon} + \frac{3}{2\varepsilon} \frac{u_\circ A_d \mu^{-\epsilon}}{(1 + m_\circ^2/\mu^2)^{\epsilon/2}} , \end{aligned} \tag{4.5}$$

$$\begin{aligned} Z_{\Phi\tilde{\Phi}}(u_\circ, m_\circ^2) &= Z_{\Phi^2}(u_\circ, m_\circ^2) \\ &= 1 + \frac{n-1}{6\varepsilon} u_\circ A_d \mu^{-\varepsilon} + \frac{1}{2\varepsilon} \frac{u_\circ A_d \mu^{-\epsilon}}{(1 + m_\circ^2/\mu^2)^{\epsilon/2}} . \end{aligned} \tag{4.6}$$

The explicit form of the Z factors demonstrates the above-mentioned features of our renormalization scheme. There are contributions from $(n-1)$ Goldstone modes, independent of temperature in the whole low-temperature phase. On the contrary, the weight factor of the longitudinal mode decreases as the mass increases and finally vanishes in the coexistence limit.

From the analytic expression for the cumulants depicted in Fig. 2, we obtain unrenormalized one-loop vertex functions according to (3.12)–(3.15). These are renormalized by the Z factors given above and combining them according to (3.16) yields the renormalized result of perturbation theory for the $\mathbf{\Phi}^2$ correlation function. Separating into real and imaginary parts ($\hat{N} = \hat{N}_1 + i\hat{N}_2$), we obtain

$$2n \, \Pi(\mathbf{k}, \omega, m^2, u, \lambda, \mu) = \frac{A_d \mu^{-\varepsilon}}{u} \frac{\hat{N}(k^2/\mu^2, \omega/\lambda\mu^2, m^2, u)}{\hat{D}(k^2/\mu^2, \omega/\lambda\mu^2, m^2, u)} \tag{4.7}$$

with real functions

$$\hat{N}_1\left(\frac{k^2}{\mu^2},\frac{\omega}{\lambda\mu^2},m^2,u\right) = 6(1+\bar{x}) + \frac{n-1}{\varepsilon}u\left[(2-\bar{x}^2-\bar{y}^2)T_1\left(\frac{k^2}{\mu^2},\frac{\omega}{\lambda\mu^2}\right) - 2\bar{y}T_2\left(\frac{k^2}{\mu^2},\frac{\omega}{\lambda\mu^2}\right)\right]$$
$$-\frac{u}{\varepsilon}\left[(\bar{y}^2+\bar{x}^2-4\bar{x}-14)L_1\left(\frac{k^2}{\mu^2},\frac{\omega}{\lambda\mu^2},m^2\right) + 6\bar{y}L_2\left(\frac{k^2}{\mu^2},\frac{\omega}{\lambda\mu^2},m^2\right)\right], \tag{4.8}$$

$$\hat{N}_2\left(\frac{k^2}{\mu^2},\frac{\omega}{\lambda\mu^2},m^2,u\right) = 6\bar{y} + \frac{n-1}{\varepsilon}u\left[2\bar{y}T_1\left(\frac{k^2}{\mu^2},\frac{\omega}{\lambda\mu^2}\right) - (\bar{x}^2+\bar{y}^2)T_2\left(\frac{k^2}{\mu^2},\frac{\omega}{\lambda\mu^2}\right)\right]$$
$$+\frac{u}{\varepsilon}\left[6\bar{y}L_1\left(\frac{k^2}{\mu^2},\frac{\omega}{\lambda\mu^2},m^2\right) - (4-4\bar{x}+\bar{x}^2+\bar{y}^2)L_2\left(\frac{k^2}{\mu^2},\frac{\omega}{\lambda\mu^2},m^2\right)\right], \tag{4.9}$$

$$\hat{D}\left(\frac{k^2}{\mu^2},\frac{\omega}{\lambda\mu^2},m^2,u\right) = (1+\bar{x})^2+\bar{y}^2 + \frac{n-1}{\varepsilon}\frac{u}{3}\left[(1+\bar{x})T_1\left(\frac{k^2}{\mu^2},\frac{\omega}{\lambda\mu^2}\right) - \bar{y}T_2\left(\frac{k^2}{\mu^2},\frac{\omega}{\lambda\mu^2}\right)\right]$$
$$+\frac{u}{\varepsilon}\left[3(1+\bar{x})L_1\left(\frac{k^2}{\mu^2},\frac{\omega}{\lambda\mu^2},m^2\right) - 3\bar{y}L_2\left(\frac{k^2}{\mu^2},\frac{\omega}{\lambda\mu^2},m^2\right)\right], \tag{4.10}$$

and $\bar{x} = k^2/(\mu^2 m^2)$, $\bar{y} = \omega/(\lambda\mu^2 m^2)$.

As shown in Appendix B, the integration of the transverse-order parameter bubble can be performed analytically and expressed by the hypergeometric function F.[32] The following abbreviations are used in (4.7):

$$T_1\left(\frac{k^2}{\mu^2},\frac{\omega}{\lambda\mu^2}\right) + iT_2\left(\frac{k^2}{\mu^2},\frac{\omega}{\lambda\mu^2}\right) = 1 - \left\{\left(\frac{\lambda k^2 - i\omega}{2\lambda\mu^2}\right)^{-\varepsilon/2} F\left(1-\varepsilon/2,\varepsilon/2,2-\varepsilon/2,\frac{1}{2}\frac{\lambda k^2}{\lambda k^2 - i\omega}\right)\right\}. \tag{4.11}$$

In case of the longitudinal order-parameter bubble, we are left with a parameter integral

$$L_1\left(\frac{k^2}{\mu^2},\frac{\omega}{\lambda\mu^2},m^2\right) + iL_2\left(\frac{k^2}{\mu^2},\frac{\omega}{\lambda\mu^2},m^2\right) = \left[(1+m^2)^{-\varepsilon/2} - (1-\varepsilon/2)\int_0^1 ds\left[m^2 + \frac{\lambda k^2 - i\omega}{2\lambda\mu^2}s - \frac{k^2}{4\mu^2}s^2\right]^{-\varepsilon/2}\right], \tag{4.12}$$

which in the case ($k = 0$) also can be evaluated analytically (see Appendix B). For completeness, we note that additive renormalization is achieved by

$$A^{(1,1)}_{(0,0)} = -(A_d\mu^{-\epsilon}/\lambda\epsilon)\left[n - 1 + (1+m^2)^{-\epsilon/2}\right].$$

Equation (4.7) is the main result of our perturbation theory for the Φ^2 – correlation function including fluctuation contributions in the low-temperature phase at finite frequency and wave vector.

V. RENORMALIZATION GROUP EQUATION AND SCALING BEHAVIOR

A. Renormalization-group equation

The renormalization-group differential equation is obtained from the requirement that unrenormalized quantities be independent of the wave number scale μ;[26] $\mu\frac{d}{d\mu}\,{}_\circ\Gamma^{(\tilde{M},M)}_{(\tilde{N},N)} = 0$. Switching to renormalized quantities yields a first-order partial differential equation

$$\left[\mu\frac{\partial}{\partial\mu} + m^2(-2+\zeta_m)\frac{\partial}{\partial m^2} + u(-\epsilon+\zeta_u)\frac{\partial}{\partial u} + \lambda\zeta_\lambda\frac{\partial}{\partial\lambda} - \tilde{M}\zeta_{\Phi\tilde{\Phi}} - M\zeta_{\Phi^2} + \frac{\tilde{N}}{2}\zeta_{\tilde{\sigma}} + \frac{N}{2}\zeta_\sigma\right]\Gamma^{(\tilde{M},M)}_{(\tilde{N},N)}$$
$$= \delta_{1,\tilde{M}}\delta_{1,M}\delta_{0,\tilde{N}}\delta_{0,N}\,B\,. \tag{5.1}$$

The ζ functions appearing in the coefficients of Eq. (5.1) and the inhomogeneity B are μ derivatives of the Z factors

$$\zeta_p = \mu\frac{\partial}{\partial\mu}\ln Z_p^{-1}\Big|_\circ\,, \qquad p\in\{m,u,\lambda\}\,, \tag{5.2}$$

$$\zeta_\Psi = \mu\frac{\partial}{\partial\mu}\ln Z_\Psi\Big|_\circ\,, \qquad \Psi\in\{\sigma,\tilde{\sigma},\Phi^2,\Phi\tilde{\Phi}\}\,, \tag{5.3}$$

$$B = -Z_{\Phi\tilde{\Phi}}Z_{\Phi^2}\left(\mu\frac{d}{d\mu}\right)Z^{-1}_{\Phi\tilde{\Phi}}Z^{-1}_{\Phi^2}\,A^{(1,1)}_{(0,0)}\Big|_\circ\,. \tag{5.4}$$

Here the symbol $|_\circ$ indicates that the derivatives have to be taken at fixed values of the unrenormalized parameters $m_\circ, u_\circ, \lambda_\circ$. Dimensional analysis yields[26]

$$\Gamma^{(\tilde{M},M)}_{(\tilde{N},N)} = \mu^{d_L}\,\lambda_\circ^{1-\tilde{M}-M}\,\hat{\Gamma}^{(\tilde{M},M)}_{(\tilde{N},N)}\,, \tag{5.5}$$

where $d_L = -(d/2)(\tilde{N}+N-2)+2-\tilde{N}+N-2\tilde{M}-4M$ denotes the μ dimension of the vertex functions, and quantities with a "hat" are dimensionsless henceforth.

The renormalization-group equation (5.1) can be integrated by the method of characteristics, yielding for dimensionless vertex functions (5.5)

$$\hat{\Gamma}^{(\tilde{M},M)}_{(\tilde{N},N)}\left(\frac{\{\mathbf{k}\}}{\mu},\frac{\{\omega\}}{\lambda\mu^2},m^2,u\right)=\exp\left[\int_1^l[(1-\tilde{M}-M)\zeta_\lambda(l')+d_L]\frac{dl'}{l'}\right]$$
$$\times\exp\left[\int_1^l\left(-\tilde{M}\zeta_{\Phi\tilde{\Phi}}(l')-M\zeta_{\Phi^2}(l')+\frac{\tilde{N}}{2}\zeta_{\tilde{\sigma}}(l')+\frac{N}{2}\zeta_\sigma(l')\right)\frac{dl'}{l'}\right]$$
$$\times\hat{\Gamma}^{(\tilde{M},M)}_{(\tilde{N},N)}\left(\frac{\{\mathbf{k}\}}{\mu(l)},\frac{\{\omega\}}{\lambda(l)\mu^2(l)},m^2(l),u(l)\right)+\delta_{1,\tilde{M}}\delta_{1,M}\delta_{0,\tilde{N}}\delta_{0,N}\,A_d\,r(l)\,,\tag{5.6}$$

where the arguments $\{\mathbf{k}\}$ and $\{\omega\}$ are sets of wave vectors and frequencies. The two exponentials steming from the dimensionality of the vertex function and the field renormalizations, respectively, constitute the exponent function. The vertex function on the right-hand side, depending on external frequencies and wave vectors explicitly is called amplitude function. An arbitrary scale parameter l induces linear variation of an effective wave number scale $\mu(l)=\mu l$. The characteristic functions $u(l),m(l)$, and $\lambda(l)$ are the solutions of the flow equations

$$\begin{aligned}l\frac{du(l)}{dl}&=u(l)\,\left[-\epsilon+\zeta_u(u(l),m(l))\right],\\ l\frac{dm(l)}{dl}&=\frac{m(l)}{2}\,\left[-2+\zeta_m(u(l),m(l))\right],\\ l\frac{d\lambda(l)}{dl}&=\lambda(l)\,\zeta_\lambda\big(u(l),m(l)\big)\,,\end{aligned}\tag{5.7}$$

with initial conditions $u(1)=u$, $m(1)=m$, $\lambda(1)=\lambda$. Additive and multiplicative renormalization of composite order parameter fields generate two more characteristics

$$\begin{aligned}r(l)&=\int_1^l\hat{B}_{\Phi^2}\big(u(l'),m(l')\big)\frac{s(l')}{l'^\epsilon}\frac{dl'}{l'}\,,\\ \hat{B}_{\Phi^2}&=-\frac{\mu^\epsilon\lambda}{A_d}B\end{aligned}\tag{5.8}$$

$$s(l)=\exp\left[-\int_1^l 2\zeta_{\Phi^2}\big(u(l'),m(l')\big)\frac{dl'}{l'}\right],\tag{5.9}$$

which alternatively can be defined as solutions of two further flow equations

$$\begin{aligned}l\tfrac{ds(l)}{dl}&=-2\,s(l)\,\zeta_{\Phi^2}\big(u(l),m(l)\big)\,,\quad s(1)=1\,,\\ l\tfrac{dr(l)}{dl}&=l^{-\epsilon}\,s(l)\,\hat{B}_{\Phi^2}\big(u(l),m(l)\big)\,,\quad r(1)=0.\end{aligned}\tag{5.10}$$

The flow equations form a set of coupled, nonlinear differential equations, for which no complete analytic solution is available. Therefore we give solutions obtained by numerical integration combined with analytic investigation of limiting behavior.

B. Asymptotic solution of the flow equations

The essential feature of the flow equations in our extended renormalization scheme is their dependence on the initial value m. Because m serves as temperature variable, it is important to determine this dependence quantitatively. Since we are interested in the properties near the phase transition, we restrict ourselves in the following discussion to a temperature range below T_I, which correponds to values $0<m\lesssim 0.1$. Under this assumption, the flow of the coupling constant, starting from $l=1$, reveals for decreasing l a plateau, i.e., $u(l)\simeq u^*_H$, at the value of the Heisenberg fixed point which is the solution of the equation $\zeta_u\big(u^*_H,0\big)=\varepsilon$. In this parameter range (values of m and l), the ζ functions acquire their critical Heisenberg fixed point values

$$\zeta_x(u(l),m(l))\simeq\zeta_x\big(u^*_H,0\big)\equiv\zeta^*_x\qquad\text{for all}\quad x\in\{u,m,\lambda,\sigma,\Phi^2\}\,,\tag{5.11}$$

$$\hat{B}_{\Phi^2}(u(l),m(l))\simeq\hat{B}_{\Phi^2}\big(u^*_H,0\big)\equiv\hat{B}^*_{\Phi^2}.\tag{5.12}$$

Setting $u(1)=u^*_H$, the flow equations can be easily integrated, yielding the initial behavior

$$\begin{aligned}u(l)&=u^*_H\,,\\ m^2(l)&=m^2l^{-2+\epsilon-\eta}\,,&\eta&=-\zeta^*_\sigma\,,\\ \lambda(l)&=\lambda l^{z-2}\,,&z&=2+\zeta^*_\lambda\,,\\ s(l)&=l^{\epsilon-\alpha/\nu}\,,&\alpha/\nu&=2\zeta^*_{\Phi^2}+\varepsilon\,,\\ r(l)&=\tfrac{\nu}{\alpha}\hat{B}^*_{\Phi^2}\big(1-l^{-\alpha/\nu}\big)\,,&\nu&=1/(2+\zeta^*_{\Phi^2})\,.\end{aligned}\tag{5.13}$$

Note that critical exponents are determined in the usual way by the Heisenberg fixed point values of the ζ functions. Due to the negative l-power law in the $m(l)$ characteristic, this function increases for decreasing l. No matter how small (but still finite) the initial value of m is, its flow-dependent counterpart $m(l)$ diverges as $l\to 0$. Thus the Heisenberg fixed point is instable, and all flow equations crossover to the stable coexistence fixed point. In this limit the coupling constant then acquires a new fixed-point value u^*_C, which is determined by $\zeta_u\big(u^*_C,\infty\big)=\varepsilon$. Again, in the coexistence fixed-point regime the ζ functions are mere constants, which are derived in Appendix A and lead to the following asymptotic behavior

$$\begin{aligned}u(l)&=u^*_C=6\varepsilon/(n-1)\,,&\zeta_u\big(u^*_C,\infty\big)&=\varepsilon\,,\\ m^2(l)&\propto l^{-2+\varepsilon}\,,&\zeta_m\big(u^*_C,\infty\big)&=\varepsilon\,,\\ \lambda(l)&\propto l^0\,,&\zeta_\lambda\big(u^*_C,\infty\big)&=0\,,\\ s(l)&\propto l^{2\varepsilon}\,,&\zeta_{\Phi^2}\big(u^*_C,\infty\big)&=-\varepsilon\,,\\ r(l)&=\text{const}+\text{const}\,l^\epsilon\,,&\hat{B}_{\Phi^2}\big(u^*_C,\infty\big)&=n-1\,.\end{aligned}\tag{5.14}$$

The l-power laws of the characteristics are determined by the coexistence fixed point. The coefficients of proportionality, left out in (5.14), are functions of m, which in the range $m<0.1$ follow power laws with Heisenberg exponents.

TABLE III. Asymptotic behavior of the homogeneous parts of the characteristic functions, with constants $\tilde{M}, \tilde{\Lambda}, \tilde{S}, \tilde{R}$.

	$l_s \to \infty$	$l_s \to 0$
$U(l_s) =$	u_H^*	u_C^*
$M^2(l_s) =$	$l_s^{-2+\epsilon-\eta}$	$\tilde{M}\, {l_s}^{-2+\epsilon}$
$\Lambda(l_s) =$	1	$\tilde{\Lambda}\, {l_s}^{2-z}$
$S(l_s) =$	1	$\tilde{S}\, {l_s}^{\epsilon+\alpha/\nu}$
$R(l_s) =$	$\frac{\nu}{\alpha}\hat{B}^*_{\Phi^2}$	$l_s^{\alpha/\nu}\left(\tilde{R} + \frac{n-1}{\epsilon}\tilde{S}\, {l_s}^{\epsilon} + \ldots\right)$

C. Universal crossover

So far, we investigated the asymptotic behavior of the characteristics at the instable Heisenberg fixed point and the stable coexistence fixed point. In the crossover regime between both limits, the coupled flow equations in general cannot be solved analytically due to the nonlinearities. Following an obvious intuition, the characteristics stick to their Heisenberg asymptotics the longer the closer the temperature to the transition point. More precisely, the crossover of the characteristic functions, which takes place at smaller values of l for decreasing m, coalesces on a unique functional flow when we use the scaled flow parameter

$$l_s = \frac{l}{m^{2/(2-\epsilon+\eta)}} \tag{5.15}$$

instead of l itself. Thus, in the investigated parameter range ($m < 0.1$), the characteristic functions, which depend on l and m are homogeneous functions

$$\begin{aligned} &u(l) = U(l_s) \quad , \quad m^2(l) = M^2(l_s), \\ &\lambda(l) = \lambda l^{z-2}\Lambda(l_s) \quad , \end{aligned} \tag{5.16}$$

$$s(l) = l^{\epsilon-\alpha/\nu}S(l_s) \quad \text{and} \quad r(l) = \frac{\nu}{\alpha}\hat{B}^*_{\Phi^2} - l^{-\alpha/\nu}R(l_s). \tag{5.17}$$

For convenience we summarize the asymptotic behavior of these homogeneous functions in the T_I limit ($l_s \to \infty$) and in the coexistence limit ($l_s \to 0$) in Table III .

We close this section by giving explicit expression for the ζ functions. In one-loop order the nonvanishing are

$$\begin{aligned} \zeta_u(u(l), m(l)) &= \zeta_m(u(l), m(l)) = \frac{n-1}{6}u(l) \\ &\quad + \frac{3}{2}\frac{u(l)}{[1+m^2(l)]^{1+\epsilon/2}}, \\ \zeta_{\Phi^2}(u(l), m(l)) &= -\frac{n-1}{6}u(l) - \frac{1}{2}\frac{u(l)}{[1+m^2(l)]^{1+\epsilon/2}}, \\ \hat{B}_{\Phi^2}(u(l), m(l)) &= n - 1 + \frac{1}{[1+m^2(l)]^{1+\epsilon/2}}. \end{aligned} \tag{5.18}$$

From our discussion in Appendix A, we know that the one-loop order already provides an exact description of the coexistence limit. However, in the critical region a one-loop theory might be too crude. For example the specific-heat exponent $\alpha = \frac{4-n}{n+8}\frac{\epsilon}{2}$ would be positive for $n = 2$ and $d = 3$, leading to a divergent specific heat. This is in contrast with higher loop calculations and experimental findings, indicating a small but negative value of α. The description of the critical region can be improved by using ζ functions obtained by Borel resummation directly for $\epsilon = 1$.[33] Originally, these resummed functions do not take into account the crossover to the coexistence limit. In order to achieve the extrapolation between the resummed critical limit on the one side, and the coexistence limit exactly contained in an one-loop order on the other side, one can be led by the following notion. All contributions beyond the one-loop order have to disappear in the coexistence limit. Generalizing the structure of the vanishing contributions of the one-loop terms to the higher-order terms, we arrive at the following expressions

$$\begin{aligned} \zeta_u(u(l), m(l)) &= \frac{n-1}{6}u(l) + \frac{3}{2}\frac{u(l)}{[1+m^2(l)]^{1.5}} + \frac{n+8}{6}\frac{\tilde{a}_4 - \tilde{a}_5}{1+\tilde{a}_5 u(l)/[1+m^2(l)]^{1.5}}\left(\frac{u(l)}{[1+m^2(l)]^{1.5}}\right)^2, \\ \zeta_\sigma(u(l), m(l)) &= -\frac{n+2}{72}\left(\frac{u(l)}{[1+m^2(l)]^{1.5}}\right)^2 + \frac{\tilde{a}_3}{24^2}\left(\frac{u(l)}{[1+m^2(l)]^{1.5}}\right)^3, \\ \zeta_{\Phi^2}(u(l), m(l)) &= -\frac{n-1}{6}u(l) - \frac{1}{2}\frac{u(l)}{[1+m^2(l)]^{1.5}} + 5\frac{n+2}{72}\left(\frac{u(l)}{[1+m^2(l)]^{1.5}}\right)^2 \\ &\quad - \frac{\tilde{a}_1}{24^2}\left(\frac{u(l)}{[1+m^2(l)]^{1.5}}\right)^3 + \frac{\tilde{a}_2}{24^3}\left(\frac{u(l)}{[1+m^2(l)]^{1.5}}\right)^4. \end{aligned} \tag{5.19}$$

The constants $\tilde{a}_j = a_j/24 \quad (j = 1, \ldots, 5)$, where the a_j are given in Table 2 of Ref. 33. In Fig. 3, we compare the scaled flow of the coupling constant obtained from the one loop and the resummed ζ functions, respectively. An obvious alteration in the latter one is its increased Heisenberg fixed-point value, leading, e.g., to improved values of critical exponents compared with their one-loop values.

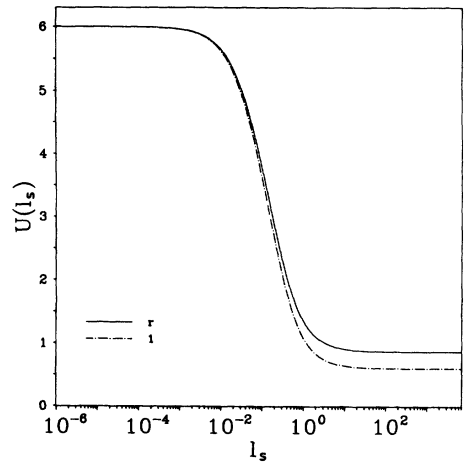

FIG. 3. Flow of the coupling constant $U(l_s)$, for an ($n = 2$)-component system and space dimension $d = 3$. The lower and upper curve correspond to the one-loop and resummed ζ functions, respectively.

VI. SCALING LAWS OF CRITICAL ULTRASOUND

A. Scaling behavior

The generalized scaling transformation of the Φ^2 correlation function reads

$$\frac{2n}{A_d}\hat{\Pi}\left(\frac{\mathbf{k}}{\mu},\frac{\omega}{\lambda\mu^2},m^2,u\right) = l^{-\epsilon}s(l)\,\frac{2n}{A_d}\hat{\Pi}\left(\frac{\mathbf{k}}{\mu(l)},\frac{\omega}{\lambda(l)\mu^2(l)},m^2(l),u(l)\right) - r(l)\,, \tag{6.1}$$

where $\hat{\Pi}$ is the renormalized and dimensionless counterpart of $\overset{\circ}{\Pi}$. The scale parameter l, introduced by the integration of the renormalization-group equation is related to physical quantities by means of a matching condition

$$\left(\frac{\omega}{\lambda(l)\mu^2(l)}\right)^2 + \left(\frac{\mathbf{k}^2}{\mu^2(l)}\right)^2 = 1\,, \tag{6.2}$$

which also prevents the right-hand side of the generalized scaling law (6.1) from being infrared singular. Inversion of (6.2) renders the flow parameter l a function of frequency and wave number $l(\omega,k)$.

To reveal scaling behavior within our theory, one has to prove that quantities as the Φ^2 correlation function are homogeneous functions of their arguments. Inserting $\lambda(l)$ from Eq. (5.16) and using the definitions of the correlation length and the characteristic frequency

$$\xi = \mu^{-1}\,m^{-2/(2-\epsilon+\eta)},\quad \omega_{\rm ch} = \lambda\mu^2\,m^{2z/(2-\epsilon+\eta)}\,, \tag{6.3}$$

Eq. (6.2) turns into an equation for the scaled flow parameter l_s with the result

$$l_s = L(k\xi,\omega/\omega_{\rm ch})\,. \tag{6.4}$$

Thus the scaled flow parameter is a function L of the scaling variables $k\xi$ and $\omega/\omega_{\rm ch}$ only. With the help of the functions defined in (5.16), we are now ready to obtain from Eq. (6.1) the scaling law for the renormalized Φ^2 correlation function

$$\frac{2n}{A_d}\hat{\Pi}\left(\frac{\mathbf{k}}{\mu},\frac{\omega}{\lambda\mu^2},m^2,u\right) = -\frac{\nu}{\alpha}\hat{B}^*_{\Phi^2} + m^{-\alpha/\beta}\,P\left(k\xi,\omega/\omega_{\rm ch}\right)\,, \tag{6.5}$$

with the scaling function $P(x,y)$ given by

$$P(x,y) = L^{-\alpha/\nu}(x,y)\left[R(L(x,y)) + S(L(x,y))\,\frac{2n}{A_d}\hat{\Pi}\left(\frac{x}{L(x,y)},\frac{y}{L^z(x,y)\Lambda(L(x,y))},M^2(L(x,y)),U(L(x,y))\right)\right]. \tag{6.6}$$

Equations (6.5) and (6.6) are central results of our investigation of the scaling behavior within the extended renormalization scheme. In the following we discuss these results in more detail.

B. Scaling functions

First we turn to the coexistence limit, where we know the flows of all characteristics and the leading terms of the amplitude function. Inserting all these informations into Eq. (6.6) we obtain for $x,y \to 0$

$$P(x,y) \to \tilde{R} + i\frac{n-1}{\varepsilon}\frac{\tilde{S}}{\tilde{\Lambda}\tilde{M}}\,y + \mathcal{O}(x^2,y^{2-\epsilon/2})\,. \tag{6.7}$$

The imaginary part of $P(x,y)$ vanishes with a linear power of y, which will have important consequences for the sound attenuation. In case of the real part the constant $\tilde{R}$ is left and we retrieve the asymptotic scaling law of the specific heat

$$\frac{2n}{A_d}\hat{\Pi}(0,0,m^2,u) = -\frac{\nu}{\alpha}\hat{B}^*_{\Phi^2} + \tilde{R}\,m^{-\alpha/\beta}\,. \tag{6.8}$$

Next we turn to the critical point limit $m \to 0$. Since now $l_s \to \infty$, the characteristics are in the Heisenberg fixed-point regime. For further applications, the asymptotic behavior of the Φ^2 correlation function is of special interest for $k \equiv 0$

$$\frac{2n}{A_d}\hat{\Pi}\left(0,\frac{\omega}{\lambda\mu^2},m^2\to 0,u\right) + \frac{\nu}{\alpha}\hat{B}^*_{\Phi^2} \propto \left(\frac{\omega}{\lambda\mu^2}\right)^{-\alpha/(z\nu)}\,, \tag{6.9}$$

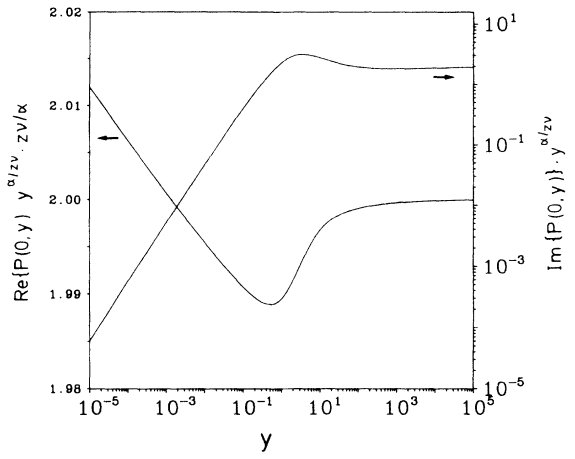

FIG. 4. Scaling functions $\mathrm{Im}\{P(0,y)\}y^{\alpha/z\nu}$ and $\mathrm{Re}\{P(0,y)\}y^{\alpha/z\nu}z\nu/\alpha$ for $n = 2$. The imaginary part is shown in a double logarithmic plot (right ordinate) and the real part with linear ordinate.

satisfying a universal power law in frequency.

We now want to illustrate the afore-mentioned features of our results. Since our treatment strongly emphasizes the scaling properties, we offer a graphical representation of the scaling functions. Removing the T_I asymptotics of $P(0,y)$ through multiplication of a factor $y^{\alpha/z\nu}$, we obtain scaling functions for the real and imaginary part, which become constant as $y \to \infty$. In Fig. 4, we display the case $n = 2$, $d = 3$. The scaling function of the real part, which has been additionally multiplied by the factor ν/α displays a weak minimum and a logarithmic divergence for small y (note the linear scale on the left ordinate). The scaling function of the imaginary part displays a clear maximum, the amplitude of which has about double value compared to the critical asymptotic amplitude. The power-law behavior for small y according to Eq. (6.7) is also evidenced in the double logarithmic plot of Fig. 4 (note the logarithmic scale on the right ordinate).

C. Scaling law of sound attenuation and velocity

Our primary goal is the coefficient of critical sound attenuation, which according to Eq. (2.19) takes the form (without background D_κ)

$$\alpha(\mathbf{k},\omega,\kappa) = \frac{\tilde{\alpha}(k/\mu,\omega/\lambda\mu^2,m)}{A(\mathbf{k},\omega,m)} \quad . \tag{6.10}$$

The frequency and temperature dependence is dominated by the factor

$$\tilde{\alpha}\left(\frac{k}{\mu},\frac{\omega}{\lambda\mu^2},m\right) \equiv \frac{\omega}{\lambda\mu^2}\,\mathrm{Im}\left\{\frac{2n}{A_d}\hat{\Pi}\left(\frac{k}{\mu},\frac{\omega}{\lambda\mu^2},m^2,u\right)\right\}, \tag{6.11}$$

and the nominator of Eq. (6.10)

$$A(\mathbf{k},\omega,m) \equiv \frac{2\,c^3(\hat{k},\omega,\kappa)}{2\,\hat{\gamma}_i^2\,c_\circ^2(\hat{k},\kappa)\,\lambda\mu^2} \times\left|1+2\hat{\gamma}_i^2\,\frac{2n}{A_d}\hat{\Pi}\left(\frac{k}{\mu},\frac{\omega}{\lambda\mu^2},m^2,u\right)\right|^2 \tag{6.12}$$

depends on the nonuniversal coupling constant $\hat{\gamma}_i$.

1. Hydrodynamic asymptotics and coexistence singularity

Inserting Eqs. (6.5) into (6.11), the scaling factor of the coefficient of sound attenuation reads

$$\tilde{\alpha}\left(\frac{k}{\mu},\frac{\omega}{\lambda\mu^2},m\right) = \left(\frac{\omega}{\lambda\mu^2}\right)^2 m^{-(\alpha+z\nu)/\beta}\,g\left(k\xi,\omega/\omega_{\mathrm{ch}}\right), \tag{6.13}$$

where the scaling function $g(x,y)$ is given by

$$g(x,y) = y^{-1}\mathrm{Im}\{P(x,y)\} \quad . \tag{6.14}$$

Most important is the asymptotic behavior of the scaling function. Obeying Eq. (6.7) we immediately recognize that $g(0,0)$ is finite, confirming the hydrodynamic ω^2 law. This is a remarkable result because individual cumulants as discussed in Appendix A contain divergent contributions of the Goldstone modes, which, however, cancel each other in the final result for $\hat{\Pi}$. This is in accord with low-order perturbation theory[12] and with the exact solution of the spherical model.[16]

The coexistence anomalies that can be attributed to the Goldstone modes lead to a cusp singularity of the scaling function. At fixed $\frac{\lambda k^2}{\omega}$ the asymptotic behavior of the scaling function g becomes

$$g\left(k\xi,\omega/\omega_{\mathrm{ch}}\right) = a_0 - a_1(n-1)\left(\omega/\omega_{\mathrm{ch}}\right)^{1-\varepsilon/2} - a_2\left(\omega/\omega_{\mathrm{ch}}\right)^{(1-\varepsilon/2)\varepsilon/2}, \tag{6.15}$$

where a_0 to a_1 are positive constants. There is a singularity induced by the transverse modes in their direct fluctuation contribution $\propto (n-1)\left(\omega/\omega_{\mathrm{ch}}\right)^{1-\varepsilon/2}$, leading to a cusp singularity at small scaling arguments. This is in accordance with the spherical model.[16] In addition, there is an even more singular contribution of the longitudinal fluctuations $\propto [(\omega/\omega_{\mathrm{ch}})^{(1-\varepsilon/2)}]^{\varepsilon/2}$, where the $(1-\varepsilon/2)$-power law just mentioned is raised by a factor $\varepsilon/2$. This observation is not entirely surprising, because the longitudinal order parameter response function (susceptibility) becomes infrared divergent in the coexistence limit, due to its coupling to the Goldstone modes.[14] In Fig. 5, the cusp singularity of $g(0,y)$ is displayed as a function of y only, producing a significant effect.

2. Critical region

The characteristic behavior in this region is exhibited by an alternative scaling function

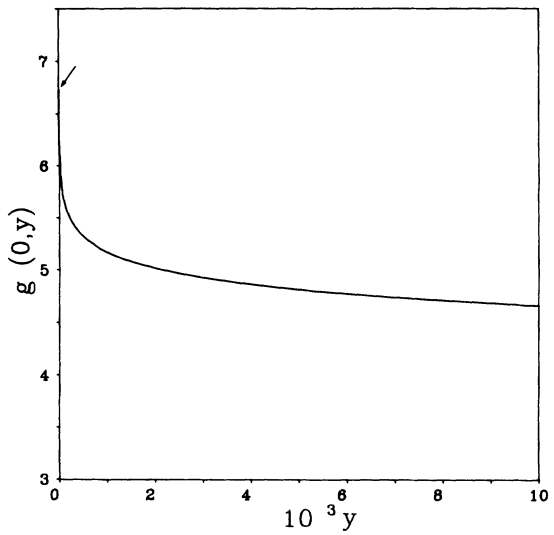

FIG. 5. Scaling function $g(0,y)$ at small scaling arguments $y = \omega/\omega_{\rm ch}$ for $n = 2$, exhibiting the Goldstone cusp singularity, the top of which is marked by the arrow.

$$G(k\xi,\omega/\omega_{\rm ch}) \equiv (\omega/\omega_{\rm ch})^{1+\alpha/(z\nu)} g(k\xi,\omega/\omega_{\rm ch}) \ , \qquad (6.16)$$

which is finite on approaching T_I. Hence, the attenuation becomes temperature independent in this limit, whereas the frequency dependence satisfies a universal power law. The scaling law can then be written in the equivalent form

$$\tilde{\alpha}\left(\frac{k}{\mu},\frac{\omega}{\lambda\mu^2},m\right) = \left(\frac{\omega}{\lambda\mu^2}\right)^{1-\alpha/(z\nu)} G\left(k\xi,\omega/\omega_{\rm ch}\right) \ . \qquad (6.17)$$

The scaling function $G(0,y)$ displays a characteristic maximum whose height decreases with increasing component number n and finally is absent in the spherical model limit.[16] Since $G(0,y) = y^{\alpha/z\nu}{\rm Im}\{P(0,y)\}$ this scaling function is identical to one of those displayed in Fig. 4 for $n = 2$ and $d = 3$. Since no analytic expressions are available for the scaling functions, we list the numerical values of the scaling function $G(0,y)$ in Table IV.

The scaling behavior of the sound velocity is more intricate to analyze. As can be seen from (2.15), the critical behavior of the sound velocity is dominated by the real part of the $\mathbf{\Phi}^2$ correlation function, whose scaling law contains a constant term as well. In Fig. 4, the ensuing scaling function is displayed for a two-component order parameter revealing only a slightly modulated structure. We prefer to describe the sound velocity as a function of temperature at fixed frequency. The sound velocity then reveals a minimum, which occurs at a lower temperature than the maximum attenuation at the same frequency.

For completeness we offer a representation of the scaling variables employing a more familiar temperature variable $\tau = (T - T_I)/T$, which is frequently used in experiments. The relation to our temperature variable m, the expectation value of the order parameter, can be deduced from definition (3.1), which is expressed by means of a critical exponent β, i.e., $m = m(1) \equiv A_m \mid \tau|^\beta$. Analogously, a critical exponent ν is defined for the correlation length $\xi \propto \mid \tau \mid^{-\nu}$, and the dynamical exponent z appears in the order parameter rate $\omega_{\rm ch} \propto \mid \tau \mid^{z\nu}$. Together with (6.3), the scaling relation $2\beta = \nu\ (2-\varepsilon+\eta)$ is recovered.[34]

3. *Anisotropic coupling of sound and order parameter modes*

Whereas isotropic coupling of sound modes and order parameter modes led to the investigation of the $\mathbf{\Phi}^2$correlation function, our discussion in Sec. II showed that there is also an anisotropic coupling, which is of inferior importance for longitudinal sound modes. However, for transverse sound modes it represents the dominant interaction, involving the lowest number of order parameter and sound modes. The critical behavior is comprised in the following order-parameter correlation function

$$\overset{\circ}{\Sigma}_\gamma(\mathbf{k},\omega) = \frac{\lambda_\circ}{n}\langle \Theta^\gamma_\circ(\mathbf{k},\omega)\ \tilde{\Theta}^\gamma_\circ(-\mathbf{k},-\omega)\rangle \ , \qquad (6.18)$$

where the composite order parameter fields are given in Eq. (2.9) and

$$\tilde{\Theta}^\gamma_\circ(\mathbf{k},\omega) \equiv \int_{\mathbf{k}_1,\omega_1} (2k_1^\gamma - k^\gamma) i \sum_{\alpha=1}^{n-1} \left\{ \tilde{\Phi}_{\circ\alpha}(\mathbf{k}_1,\omega_1)\Phi_{\circ n}(\mathbf{k}-\mathbf{k}_1,\omega-\omega_1) - \tilde{\Phi}_{\circ n}(\mathbf{k}_1,\omega_1)\Phi_{\circ\alpha}(\mathbf{k}-\mathbf{k}_1,\omega-\omega_1)\right\} . \qquad (6.19)$$

TABLE IV. Values of the scaling function $G(0,y)$ for $n = 2$ and $d = 3$, for logarithmically equidistant values of y.

$y \times 10^k =$	1.0	1.4678	2.1544	3.1623	4.6416	6.8129
$k = 3$	0.0052	0.0075	0.0108	0.0156	0.0225	0.0325
$k = 2$	0.0468	0.0674	0.0969	0.1392	0.1991	0.2838
$k = 1$	0.4020	0.5646	0.7835	1.0695	1.4270	1.8458
$k = 0$	2.2905	2.6979	2.9925	3.1235	3.0929	2.9483
$k = -1$	2.7504	2.5462	2.3622	2.2086	2.0868	1.9936
$k = -2$	1.9247	1.8755	1.8419	1.8204	1.8083	1.8032

Through the same procedure, which has been applied in case of the Φ^2 correlation function, the scaling law for this new order parameter function can be inferred

$$\frac{n}{A_d}\hat{\Sigma}_\gamma\left(\frac{\mathbf{k}}{\mu},\frac{\omega}{\lambda\mu^2},m^2,u\right) = -\frac{\nu}{\alpha^*}\hat{B}^{(6)}\left(\frac{\mathbf{k}}{\mu},\frac{\omega}{\lambda\mu^2},m^2\right) + m^{-\alpha^*/\beta}\,P_\gamma\left(\mathbf{k}\xi,\omega/\omega_{\rm ch}\right). \tag{6.20}$$

The value of the exponent $\alpha^*/\nu = -2+\varepsilon+\mathcal{O}(\varepsilon^2)$ is found from low-order perturbation theory. The asymptotic behavior of the scaling function in the coexistence limit can be determined for different orientations of the wave vector. If $\mathbf{k}$ is oriented along the direction selected by index γ we obtain

$$P_\gamma\,|_{CL} \propto \frac{(k^\gamma\xi)^2}{k^2\xi^2-(i/\tilde{\Lambda})\omega/\omega_{\rm ch}}, \quad (\mathbf{k}\parallel\mathbf{e}_\gamma)\,. \tag{6.21}$$

If $\mathbf{k}$ stands perpendicular to the γ direction ($k^\gamma = 0$), we take advantage of the simplification that occurs by setting $k\xi = 0$

$$\mathrm{Im}\left\{P_\gamma\,|_{CL}\right\} \propto \left(\omega/\omega_{\rm ch}\right)^{2-\varepsilon}, \quad (\mathbf{k}\perp\mathbf{e}_\gamma)\,. \tag{6.22}$$

The scaling behavior of the sound attenuation steming from the anisotropic coupling can be investigated by a scaling factor $\bar{\alpha}_\gamma$, defined in an analogous way as $\tilde{\alpha}$ has been defined in case of isotropic coupling. Here we have to consider the different orientations of the wave vector separately. For $\mathbf{k}\perp\mathbf{e}_\gamma$ we find the following scaling law

$$\bar{\alpha}_\gamma\left(\frac{\mathbf{k}}{\mu},\frac{\omega}{\lambda\mu^2},m\right) = \left(\frac{\omega}{\lambda\mu^2}\right)^{3-\varepsilon} m^{-[\alpha^*+z\nu(2-\varepsilon)]/\beta}\,\bar{g}_\gamma\left(\mathbf{k}\xi,\omega/\omega_{\rm ch}\right), \tag{6.23}$$

with an asymptotic frequency power law depending on dimension. Observing that the scaling function

$$\bar{g}_\gamma\left(\mathbf{k}\xi,\omega/\omega_{\rm ch}\right) = \frac{1}{(\omega/\omega_{\rm ch})^{2-\varepsilon}}\,\mathrm{Im}\left\{P_\gamma\left(\mathbf{k}\xi,\omega/\omega_{\rm ch}\right)\right\} \quad \text{for} \quad (\mathbf{k}\perp\mathbf{e}_\gamma) \tag{6.24}$$

is finite for vanishing scaling arguments, we retrieve an ω^2 law for $d=3$.

Next we consider the case where the wave vector $\mathbf{k}$ is parallel to $\mathbf{e}_\gamma$. The scaling law then reads

$$\bar{\alpha}_\gamma\left(\frac{\mathbf{k}}{\mu},\frac{\omega}{\lambda\mu^2},m\right) = \left(\frac{\omega}{\lambda\mu^2}\right)^2 m^{-(\alpha^*+z\nu)/\beta}\,\bar{g}_\gamma\left(\mathbf{k}\xi,\omega/\omega_{\rm ch}\right), \tag{6.25}$$

and the scaling function is given by

$$\bar{g}_\gamma\left(\mathbf{k}\xi,\omega/\omega_{\rm ch}\right) = \frac{1}{(\omega/\omega_{\rm ch})}\mathrm{Im}\left\{P_\gamma\left(\mathbf{k}\xi,\omega/\omega_{\rm ch}\right)\right\} \quad \text{for} \quad (\mathbf{k}\parallel\mathbf{e}_\gamma)\,. \tag{6.26}$$

The limiting behavior in the coexistence limit can be read off from the following expression:

$$\bar{g}_\gamma\left(\mathbf{k}\xi,\omega/\omega_{\rm ch}\right) \;\to\; \mathrm{Im}\left\{\frac{(k\xi)^2}{\left(\omega/\omega_{\rm ch}\right)\left[\left(k\xi\right)^2-(i/\tilde{\Lambda})\left(\omega/\omega_{\rm ch}\right)\right]}\right\}, \tag{6.27}$$

where we have used that $|\,\mathbf{k}\,| = k = k^\gamma$ for this orientation of the wave vector. Evidently, the asymptotic behavior depends on the dispersion relation $\omega(\mathbf{k})$ and for linear dispersion $\bar{g}_\gamma(0,0)$ is finite.

Finally, we give an alternative formulation of the scaling law by extracting the critical asymptotics, which takes the same form for both orientations of the wave vector

$$\bar{\alpha}_\gamma\left(\frac{\mathbf{k}}{\mu},\frac{\omega}{\lambda\mu^2},m\right) = \left(\frac{\omega}{\lambda\mu^2}\right)^{1-\alpha^*/z\nu}\bar{G}_\gamma\left(\mathbf{k}\xi,\omega/\omega_{\rm ch}\right). \tag{6.28}$$

Concerning the anisotropic coupling, the determination of the asymptotic behavior of the ensuing coefficient of attenuation already is a noteworthy achievement, which has been made possible by the utilization of the extended renormalization scheme. However, a reliable result for the crossover scaling functions only can be obtained from a two-loop perturbation theory, which presently is not available.

VII. APPLICATION OF THE THEORY TO EXPERIMENTS

This section is devoted to the application of our theory to ultrasonic measurements. The energy functional (2.2) is appropriate within the plane-wave region of the incommensurate phase. On entering the soliton regime it might be supplemented by anharmonics higher than quartic, which then are required for a description of the incommensurate modulation. Note also that the incommensurability parameter is temperature-independent in our model. These facts should be kept in mind when dealing with substances where the lock-in-transition at T_L is quite close to the incommensurate transition. In several substances, the incommensurate phase extends over a wide temperature range; therefore critical sound attenuation should be observed entirely within the plane-wave regime, and our theory is fully applicable.

Concerning the sound attenuation, the main result of our study, besides the determination of the asymptotic behavior in the critical and the hydrodynamic regime,

is the computation of the scaling functions connecting both limits. To recover the scaling functions from experimental data $\alpha_{\rm expt}$ on sound attenuation, one has to remove the nonscaling function denoted as $A(\mathbf{k},\omega,m)$ in (6.10). The importance of taking a nonscaling part into account was pointed out by Ferrell and Bhattacharjee,[35] who analyzed sound attenuation in superfluid helium-4. The scaling function $G(k\xi,\omega/\omega_{\rm ch})$ is obtained in the following way:

$$G_{\rm expt}(k\xi,\omega/\omega_{\rm ch}) = \frac{\alpha_{\rm expt}}{(\omega/\lambda\mu^2)^{1-\alpha/(z\nu)}}\, A(\mathbf{k},\omega,m)\ ; \quad (7.1)$$

it then can be compared with our theoretical result (6.16).

This procedure will be applied to Rb_2ZnCl_4, which is a well-studied member of the A_2BX_4 family.[4] Its incommensurate phase extends over more than 100 K, and the constancy of its incommensurability parameter within the plane-wave regime is remarkable.[36] Therefore the possible objections mentioned above do not apply for this substance. We analyze experiments of Hirotsu *et al.*,[10,37] who measured ultrasonic velocities and attenuation in Rb_2ZnCl_4. One experiment[37] was done at a single frequency of 10 MHz for all three longitudinal modes C_{ll} $(l = 1,2,3)$; according to this experiment, the C_{33} mode shows the strongest acoustic anomaly. In a second experiment,[10] the attenuation of the C_{33} mode was measured at several frequencies. Sample preparation and changing experimental conditions influence ultrasonic results. For the frequency $\omega = 30$ MHz, there exists an independent measurement performed by Lemanov and Esayan,[38] revealing quantitative discrepancies between the two experiments, which otherwise show the same qualitative behavior. The experimental origin of this discrepancy has not been commented on in Ref. 38. In view of these uncertainties, we restrict ourselves to the measurements of Hirotsu *et al.*[10,37]

In determining the experimental scaling function, a simplification occurs: Because the wave numbers accessible to ultrasonics are small,[39] we can set the scaling variable $k\xi \equiv 0$ to good approximation within the temperature range covered by present experiments. The scaling function thus depends only on $\omega/\omega_{\rm ch}$. After application of the procedure implied by (7.1), we obtain the experimental scaling function, depicted by the points in the insert of Fig. 6. As a first success of our theory, we recognize that the measurements at different frequencies coalesce fairly well onto a single curve. At this point we emphasize that the experimental data points have not been normalized to their asymptotic value $\alpha(T = T_I)$.

The determination of the experimental scaling function requires the knowledge of several quantities. Firstly, there are the universal critical exponents, which are given by the Heisenberg fixed point values of the previously introduced ζ functions

$$\beta = 0.3485,\quad \nu = 0.667,\quad z = 2,\quad \alpha/\nu = -0.0025\ . \quad (7.2)$$

We mention that the value of the exponent β and the negative but almost zero value of the specific-heat exponent α are confirmed by experimental investigations.[40,41] Additionally, there are the nonuniversal, substance specific quantities. From the asymptotic critical amplitude of the attenuation, the phonon order-parameter coupling $(\hat{\gamma}_3)^2 = 0.022$ and the bare sound velocity along the **c** direction $c_0(\mathbf{c},l) = 2470\,\mathrm{m/sec}$ can be inferred. The remaining parameters are the amplitude of the order parameter A_m and the frequency scale $\lambda\mu^2$, a combination of which yields the amplitude $W = \lambda\mu^2(A_m)^{z\nu/\beta}$ of the order parameter frequency $\omega_{\rm ch} = W \mid \tau \mid^{z\nu}$. Our analysis yields the value $W = 7.853 \times 10^{11}$ Hz. For a proper theoretical description, the transition temperature must be known very accurately. In the presentation of the data we use $T_I = 302.65$ K, which is 0.03 K higher than the value obtained in a mean-field analysis performed in Ref. 10.

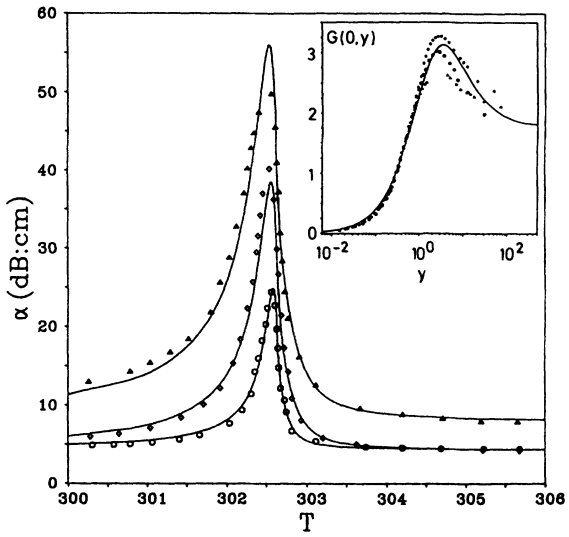

FIG. 6. Experimental attenuation in Rb_2ZnCl_4 as function of temperature for three different frequencies ○: 30 MHz, ◇: 50 MHz, △: 70 MHz in comparison with the theoretical result represented by the solid lines. The inset shows the theoretical scaling function $G(0,y)$ in the incommensurate phase for $n = 2$ (solid) vs the scaling variable $y = \omega/\omega_{\rm ch}$.

The theoretical scaling function is also indicated by the solid curve in the inset of Fig. 6. The success of our theory is evident from the observation that there is coincidence with experimental data over almost four orders of magnitude of the scaling variable. Complementary to this scaling analysis, in Fig. 6 we also show the complete coefficient of sound attenuation as a function of temperature for the above frequencies including the high-temperature phase. The result of the theory developed in this work is represented by the solid lines for each frequency separately. Since the theoretical treatment of the normal phase is much easier than for the incommensurate phase, we defer it to Appendix C.

The final question concerns the observability of the coexistence singularity (6.15) in experiments. The smallest values of y obtained experimentally are in the range $y \sim 10^{-2}$ (Fig. 6). From Fig. 5, it appears that values of y smaller by one to two orders of magnitude are required

to reveal the cusp singularity in Rb_2ZnCl_4.

Next we turn to the sound velocity, where for the C_{33} mode there exists a single measurement at 10 MHz (Ref. 37) for Rb_2ZnCl_4. Because the nonuniversal parameters are fixed for that substance by the attenuation data, our theory is now challenged to give a description without any further adjustments. In Fig. 7, the crosses show the experimental data. The solid curve represents our theoretical result, and the overall coincidence is gratifying. The minimum of the velocity actually occurs at a lower temperature than the maximum attenuation. A shift of $0.2 \sim 0.3$ K has been reported in the experiments, in agreement with our prediction.

In Brillouin scattering experiments, the elastic properties of incommensurate systems are probed in the range of frequencies higher than in ultrasonic experiments. From a measurement of the shift $\Delta\omega_B$ and the width Γ of the Brillouin line, the sound velocity and damping can be deduced in the following way

$$\Delta\omega_B = c(\hat{k},\omega,\kappa)k \quad \text{and} \quad \Gamma = D(\hat{k},\omega,\kappa)k^2 \ . \tag{7.3}$$

In a recent Brillouin experiment on K_2SeO_4 (Ref. 11) longitudinal sound modes along the **c** direction have been investigated at two different scattering angles, corresponding to two acoustic frequencies. The experimental data for the line width are shown in Fig. 8 as a function of temperature together with the theoretical result represented by the solid lines. The acoustic anomalies in K_2SeO_4 are quantitatively more pronounced than in Rb_2ZnCl_4, which is reflected by the larger value of the phonon order-parameter coupling whose magnitude is found to be $(\hat{\gamma}_3)^2 = 0.0475$. The amplitude of the characteristic order parameter frequency, being another quantity of interest, is markedly higher in this A_2BX_4 compound. The value of $W = 9.567 \times 10^{13}$ Hz is two orders of magnitude larger than in Rb_2ZnCl_4.

As a final remark, we draw attention to the fact that

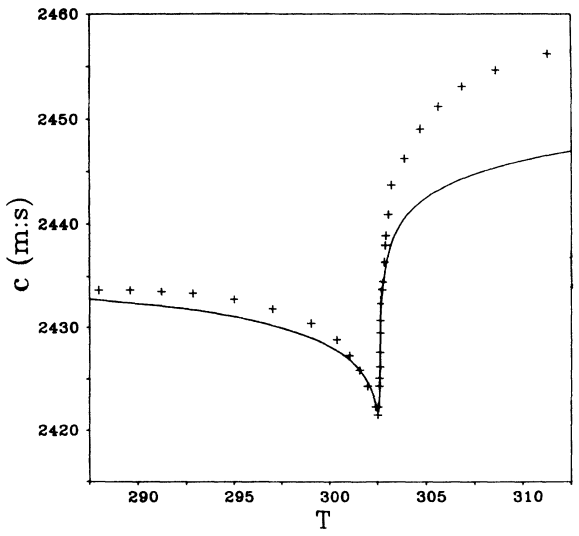

FIG. 7. Experimental (symbols) and theoretical (solid line) ultrasonic velocity at the normal-incommensurate transition of Rb_2ZnCl_4 for 10 MHz.

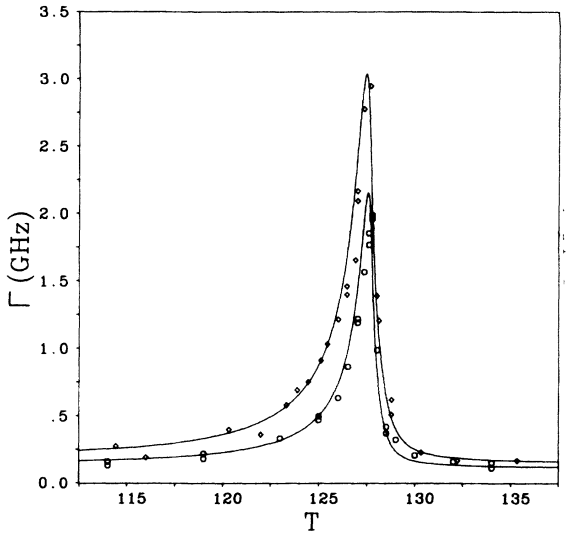

FIG. 8. Brillouin line width for longitudinal sound modes in K_2SeO_4 along the **c** direction as function of temperature. Experimental data at two scattering angles [90°(○), 180°(◇)] are shown together with the theoretical result indicated by the solid lines.

experimental findings of acoustic properties in Rb_2ZnCl_4 and K_2SeO_4 could be explained without the *ad hoc* introduction of a gap in the energy spectrum of the phason modes at zero wave number, as introduced in previous studies. First we mention the paper of Zeyher,[9] who investigated ultrasonic attenuation in incommensurate solids due to order parameter fluctuations by means of a $1/n$ expansion. Due to a subtle error a spurious nonhydrodynamic $\omega^{3/2}$ law of the attenuation coefficient was predicted, which was attributed to the Goldstone modes. Since experiments reveal a ω^2 law in the hydrodynamic regime,[10] the divergence of the viscosities responsible for the nonhydrodynamic behavior is cured by hand through introduction of a phason gap. The frequently cited[4,39] $\omega^{3/2}$ prediction may have been a source of confusion in data analysis seeking a measurable signature of the Goldstone modes.

In the work of Li *et al.*,[11] the complex elastic constants were derived, including anharmonic fluctuation contributions, which, however, are not treated consistently within a certain order of perturbation theory of critical phenomena. In consequence, no scaling behavior was derived, and infrared divergencies remain in the final result. These are removed through inclusion of a phason gap, but the authors stress that this an additional assumption not predicted by their theory.

Recently Hu *et al.*[42] presented an analysis of acoustic attenuation in Rb_2ZnCl_4 based on phenomenological scaling arguments. In the incommensurate phase, the fluctuation contribution is not determined by direct computation as in our work, but rather it is eliminated by a subtraction method. The procedure is very sensitive to the choice of auxiliary parameters, as stated by the authors. It cannot be applied to experimental data close to the transition temperature and offers no insight into

the special features of the fluctuation spectrum in the incommensurate phase.

In our theory, there is no need to introduce a phason gap in order to eliminate infrared divergences of certain perturbative contributions. As stated at the end of Sec. III, a nontrivial cancellation of these divergences occurs, which is a special feature of $O(n)$ symmetric expectation values[13] such as that required for the Φ^2 correlation function.

VIII. SUMMARY AND DISCUSSION

In this work, we have elaborated a theory of ultrasonic attenuation and velocity at normal-incommensurate phase transitions. The description is based on a dynamic model for a nonconserved, multicomponent order parameter and a phonon variable representing longitudinal and transverse sound wave propagating along high-symmetry directions. The coupling between the two degrees of freedom is quadratic in the former and linear in the latter. From this model, acoustic anomalies could be derived. The coefficient of critical sound attenuation and the sound velocity are related to a Φ^2 correlation function, which is a purely critical dynamical quantity; in the present theory, the critical dynamics belongs to the universality class of the time-dependent model A. Due to the continuous symmetry of this model, Goldstone modes appear in the phase of broken symmetry, i.e., the phason modes of the incommensurate phase.

The perturbation theory for the Φ^2 correlation function is plagued by severe infrared divergences induced by the Goldstone modes, leading to coexistence anomalies. Their proper treatment is one of the principal goals of our theory. Moreover, as it turns out, in our theory the coexistence limit is exactly tractable, from which important information can be deduced: To begin with, the Goldstone mode divergences of perturbative contributions to the Φ^2 correlation function exactly cancel. In consequence, the hydrodynamic frequency dependence of the coefficient of sound attenuation is maintained, and an asymptotic ω^2 law is recovered. Concerning the presence of coexistence anomalies, the corrections to asymptotics have to be considered. Indeed, the scaling function $g(x,y)$ exhibits a cusp singularity at small scaling variables, which is the manifest signature of the unique Goldstone modes [Eq. (6.15)]. By means of an extended renormalization scheme, it was possible for the first time to determine this coexistence anomaly of the coefficient of sound attenuation at a finite number n of components of the order parameter. Our previous studies within the spherical model led to analagous results; however, in this case one has effectively $n = \infty$.

The coexistence anomaly of the scaling function $g(x,y)$ is its outstanding feature, predicting a measurable effect. Another important property of the scaling function is that it describes the universal crossover from the hydrodynamic to the critical limit, covering several orders of magnitude of the scaling variables. In the critical limit, the attenuation becomes independent of temperature, but it satisfies a power law in frequency. This allows one to introduce a new scaling function G, differing from the previous one g only by a power law [Eq. (6.16)]; G acquires a finite amplitude in the critical limit. Thus the scaling law for the coefficient of sound attenuation can be stated in two equivalent ways [Eqs. (6.13) and (6.17)], either by separation of the hydrodynamic asymptotics and a scaling function g with a coexistence singularity, or by separation of the critical point asymptotics. The scaling function G in the latter case displays a characteristic maximum.

To obtain this detailed theoretical description of critical ultrasound at incommensurate phase transitions, it is indispensable to take order parameter fluctuations into account. Occasionally the acoustic anomalies have been separated into a relaxational part, as contained in the Landau-Khalatnikov theory, and an anharmonic contribution yielding fluctuation processes. Within our theory, both mechanisms are incorporated on an equal footing; the loop expansion avoids the need for artificially splitting the two processes. Moreover, consideration of fluctuation effects must be performed carefully because of the peculiarities induced by the Goldstone modes. Our theory allows an exact treatment of the coexistence limit. Higher-order effects appear in the crossover regime and in the critical-point limit. Utilization of the resummed ζ functions proved to be a successful attempt to incorporate the higher loop-order effects within our one-loop calculation of amplitude functions.

Proper interpretation of experiments is possible on the basis of our theory. According to the concept of universality of critical phenomena, a description of a large number of substances is possible, e.g., the members of the A_2BX_4 family. Our goal of determining the scaling functions of ultrasonic attenuation has been achieved. Application to ultrasonic experiments of Rb_2ZnCl_4 and Brillouin-scattering experiments of K_2SeO_4 convincingly demonstrates the success of our theory. Although the scaling functions g and G are equivalent, it is expedient to analyze present experiments in terms of the scaling function G. The crossover behavior predicted by our theory causes a nontrivial structure of this scaling function, i.e., the characteristic maximum of G. It would be rewarding to apply our theory to other substances as well; however, to perform a reliable analysis, experimental data with an accurate temperature resolution are required. The ultimate goal would be to reveal the coexistence anomaly in experiments. Turning our attention to the scaling function g, we must recognize that in existing experiments, the range of scaling arguments small enough for the cusp singularity to appear has unfortunately not yet been reached. To detect this Goldstone anomaly, further experimental work will be necessary. The influence of the Goldstone modes is present already in the crossover regime, but confirmation of the coexistence anomaly would be even more convincing.

Our theory allows application to other experimental probes as well, e.g., the integrated intensity of Raman scattering is related to the energy correlation function, which also can be derived from the Φ^2 correlation function within the static limit. The energy correlation function and several other dynamic correlation functions of composite order parameter fields already have been inves-

tigated theoretically by the present authors.[16,43] Finally, based on the present work, the treatment of the coexistence anomalies of more complicated systems, such as superfluid helium-4, charge-density-wave systems or liquid crystals may be possible.

ACKNOWLEDGMENT

We gratefully acknowledge support from the Deutsche Forschungsgemeinschaft (DFG) under Contract No. Schw. 348/4-2.

APPENDIX A: THEORY WITHIN THE COEXISTENCE LIMIT

In the investigation of the coexistence limit one has to take care of the fact that $m_\circ$ not only appears as mass of the longitudinal modes (3.6), but also is part of the coupling constant of third-order vertices (3.7). Employing the substitution $\tilde{s}_\circ = m_\circ \tilde{\sigma}_\circ$ and $s_\circ = m_\circ \sigma_\circ$, the dynamical functional is severely reduced in its complexity after performing the limit $m_\circ \to \infty$.[14] The true nature of the coexistence limit is revealed by a final transformation

$$\begin{aligned}\varphi_\circ(\mathbf{k},\omega) &= s_\circ(\mathbf{k},\omega) + \tfrac{1}{2}\sqrt{\tfrac{u_\circ}{3}} \int_{\mathbf{k}_1,\omega_1} \sum_\alpha \pi_\circ^\alpha(\mathbf{k}_1,\omega_1)\pi_\circ^\alpha(\mathbf{k}-\mathbf{k}_1,\omega-\omega_1) + \sqrt{\tfrac{3}{u_\circ}} A\delta(\mathbf{k})\delta(\omega) \quad , \\ \tilde{\varphi}_\circ(\mathbf{k},\omega) &= \tilde{s}_\circ(\mathbf{k},\omega) + \sqrt{\tfrac{u_\circ}{3}} \int_{\mathbf{k}_1,\omega_1} \sum_\alpha \tilde{\pi}_\circ^\alpha(\mathbf{k}_1,\omega_1)\pi_\circ^\alpha(\mathbf{k}-\mathbf{k}_1,\omega-\omega_1) \quad .\end{aligned} \tag{A1}$$

The limiting dynamical functional follows as

$$\mathcal{J}\,|_{CL}\,[\{\pi_\circ^\alpha\},\varphi_\circ,\{\tilde{\pi}_\circ^\alpha\},\tilde{\varphi}_\circ] = \int_{\mathbf{k}_1,\mathbf{k}_2}\int_{\omega_1,\omega_2}\Big[\sum_\alpha \lambda_\circ\,\tilde{\pi}_\circ^\alpha\tilde{\pi}_\circ^\alpha - \lambda_\circ\,\tilde{\varphi}_\circ\varphi_\circ - \sum_\alpha \tilde{\pi}_\circ^\alpha\big[i\omega_1 + \lambda_\circ k_1^2\big]\pi_\circ^\alpha\Big] \quad . \tag{A2}$$

The crucial point is that $\mathcal{J}\,|_{CL}$ consists only of bilinear terms discribing a Gaussian theory of the fields $\tilde{\boldsymbol{\pi}}_\circ, \tilde{\varphi}_\circ, \boldsymbol{\pi}_\circ, \varphi_\circ$. As a consequence the coexistence limit of our model is exactly soluble. For instance, from $\mathcal{J}\,|_{CL}$ the exact response functions are given by

$$\langle \pi_\circ^\alpha\,\tilde{\pi}_\circ^\beta\rangle_{\mathbf{k},\omega}\,|_{CL} = \frac{\delta_{\alpha,\beta}}{\lambda_\circ k^2 - i\omega}, \quad \langle \varphi_\circ\,\tilde{\varphi}_\circ\rangle_{\mathbf{k},\omega}\,|_{CL} = \frac{1}{\lambda_\circ} \quad . \tag{A3}$$

The cumulants required for the phonon self-energy according to (3.11) reduce to certain "$s_\circ, \boldsymbol{\pi}_\circ$" expectation values in the coexistence limit

$$\begin{aligned} {}^{\circ}_{}G^{(1,1)}_{(0,0)}|_{CL} &= \langle \boldsymbol{\pi}_\circ^2\,(\boldsymbol{\pi}_\circ\tilde{\boldsymbol{\pi}}_\circ)\rangle\big|_{CL} \quad , \\ m_\circ\,{}^{\circ}_{}G^{(1,0)}_{(0,1)}|_{CL} &= \langle s_\circ\,(\boldsymbol{\pi}_\circ\tilde{\boldsymbol{\pi}}_\circ)\rangle\big|_{CL} \quad , \\ m_\circ\,{}^{\circ}_{}G^{(0,1)}_{(1,0)}|_{CL} &= \langle \boldsymbol{\pi}_\circ^2\,\tilde{s}_\circ\rangle\big|_{CL} \quad , \\ m_\circ^2\,{}^{\circ}_{}G^{(0,0)}_{(1,1)}|_{CL} &= \langle s_\circ\,\tilde{s}_\circ\rangle|_{CL} \quad . \end{aligned} \tag{A4}$$

From $\mathcal{J}\,|_{CL}$ these expectation values are easily obtained. For $\langle \boldsymbol{\pi}_\circ^2\,(\boldsymbol{\pi}_\circ\tilde{\boldsymbol{\pi}}_\circ)\rangle\big|_{CL}$ there is only a one-loop contribution because the asymptotic functional has no vertices. Using the definition of the fields $\varphi_\circ, \tilde{\varphi}_\circ$ (A1) together with (A3) yields the longitudinal response function

$$\langle s_\circ\tilde{s}_\circ\rangle|_{CL} = \frac{1}{\lambda_\circ} + \frac{u_\circ}{6}\,\langle \boldsymbol{\pi}_\circ^2(\boldsymbol{\pi}_\circ\tilde{\boldsymbol{\pi}}_\circ)\rangle\big|_{CL} \quad . \tag{A5}$$

Analogously we find

$$\begin{aligned}&\langle \boldsymbol{\pi}_\circ^2\,\tilde{s}_\circ\rangle\big|_{CL} + 2\,\langle s_\circ\,(\boldsymbol{\pi}_\circ\tilde{\boldsymbol{\pi}}_\circ)\rangle|_{CL} \\ &\qquad = -2\sqrt{\frac{u_\circ}{3}}\,\langle \boldsymbol{\pi}_\circ^2\,(\boldsymbol{\pi}_\circ\tilde{\boldsymbol{\pi}}_\circ)\rangle\big|_{CL} \quad .\end{aligned} \tag{A6}$$

Inserting these expectation values into (3.11) leads to result (3.17) of Sec. III for the $\boldsymbol{\Phi}^2$ correlation function. In this derivation an important feature of $O(n)$-symmetric functions becomes obvious. It is the cancellation of the multiple contribution of the infrared divergent transverse order parameter bubble appearing in the cumulants of (A4).

From (A4) we learn that in the limit $m_\circ \to \infty$ the cumulants can be determined exactly. Deriving a sufficient set of cumulants and obeying the structure of the asymptotic functional (A2), the renormalization constants of the theory can be obtained. Thus we recognize that there is no renormalization of order parameter fields and the relaxation constant;[14] $Z_\sigma\,|_{CL} = Z_{\tilde{\sigma}}\,|_{CL} = Z_\pi\,|_{CL} = Z_{\tilde{\pi}}\,|_{CL} = Z_\lambda\,|_{CL} = 1$. The nontrivial Z factors are identical, namely,

$$\begin{aligned} Z_u\,|_{CL} = Z_m\,|_{CL} &= Z_{\Phi^2}\,|_{CL} = Z_{\Phi\tilde{\Phi}}\,|_{CL} \\ &= 1 + \frac{n-1}{6\varepsilon}u_\circ A_d\mu^{-\epsilon} \quad , \end{aligned} \tag{A7}$$

and coincide with the one-loop expressions of Sec. IV, when taking the limit $m_\circ \to \infty$ in the latter ones. In terms of the renormalized coupling constant the Z factors read[13]

$$Z_u^{-1}\,|_{CL} = 1 - \frac{n-1}{6\varepsilon}u. \tag{A8}$$

By inserting these Z factors into the definitions of the vertex functions one easily reassures that these are indeed free of ε poles provided the additive renormalization

$$A^{(1,1)}_{(0,0)} = -\frac{A_d\mu^{-\epsilon}}{\lambda_\circ\varepsilon} Z_u\,|_{CL}\,(n-1) \tag{A9}$$

is taken into account. The ζ functions can be performed in closed form. Several ones are zero $\zeta_\sigma\,|_{CL} = \zeta_{\tilde{\sigma}}\,|_{CL} = \zeta_\pi\,|_{CL} = \zeta_{\tilde{\pi}}\,|_{CL} = \zeta_\lambda\,|_{CL} = 0$, and the nonvanishing ones are

$$\zeta_u\,|_{CL}=\zeta_m\,|_{CL}=-\zeta_{\Phi^2}\,|_{CL}=-\zeta_{\Phi\tilde{\Phi}}\,|_{CL}=\frac{n-1}{6}u\,,$$
$$\hat{B}_{\Phi^2}\,|_{CL}=n-1\,. \tag{A10}$$

With $u_C^*=6\epsilon/(n-1)$ the fixed point values of the ζ functions are determined to be those denoted in (5.14). Note that, while the coupling constant acquires its finite fixed-point value, the flow-dependent counterpart of the renormalized temperature variable diverges as $m(l)\propto l^{-2+\epsilon}$ for $l\to 0$. Thus we are in agreement with the assumed ($m_\circ\to\infty$) limit underlying the discussion of this appendix. Within the renormalized theory we retrieve an asymptotic behavior corresponding in a self-consistent fashion to the limiting structure of the bare theory.

Finally we remark that an interesting connection can be established between the coexistence limit of our model and the spherical model ($n\to\infty$), investigated in Ref. 16. Namely, the same expectation values of transverse and longitudinal fields appear in both limits (compare Eqs. (3.11) and (A4) of the present work to Eq. (3.20) of Ref. 16). Indeed, if we send $n\to\infty$ in our present results we recover the analogous expression of the spherical model, when we consider the coexistence limit ($\mathbf{k},\omega\to 0$). Especially the cusp singularity of the scaling function is found in both cases.

APPENDIX B: INTEGRATION OF ORDER-PARAMETER BUBBLES

The transverse and longitudinal order-parameter bubbles appearing in Fig. 2 read

$$\overset{\circ}{I}_\pi(\mathbf{k},\omega)=\int\frac{d^d\mathbf{k}_1}{(2\pi)^d}\int\frac{d\omega_1}{2\pi}\,\langle\pi_\circ^1\,\tilde{\pi}_\circ^1\rangle_{\mathbf{k}+\mathbf{k}_1,\omega+\omega_1}\,\langle\pi_\circ^1\,\pi_\circ^1\rangle_{\mathbf{k}_1,\omega_1}\quad, \tag{B1}$$

$$\overset{\circ}{I}_\sigma(\mathbf{k},\omega)=\int\frac{d^d\mathbf{k}_1}{(2\pi)^d}\int\frac{d\omega_1}{2\pi}\,\langle\sigma_\circ\,\tilde{\sigma}_\circ\rangle_{\mathbf{k}+\mathbf{k}_1,\omega+\omega_1}\,\langle\sigma_\circ\,\sigma_\circ\rangle_{\mathbf{k}_1,\omega_1}\quad, \tag{B2}$$

where the bare correlation propagators are given by a fluctuation-dissipation theorem. The frequency integration is performed by residue calculus. The remaining wave vector integration can be reduced with the help of a Feynman parametrization

$$\frac{1}{A^aB^b}=\frac{\Gamma(a+b)}{\Gamma(a)\Gamma(b)}\int_0^1 ds\frac{s^{(a-1)}(1-s)^{(b-1)}}{\left[sA+(1-s)B\right]^{(a+b)}} \tag{B3}$$

to a prototype integral, which can be performed according to the procedure of dimensional regularization[28]

$$\int\frac{d^d\mathbf{k}_1}{(2\pi)^d}\frac{1}{\left(M^2+2\mathbf{k}\mathbf{k}_1+\mathbf{k}_1^2\right)^p}=\frac{S_d}{2}\frac{\Gamma(p-d/2)\Gamma(d/2)}{\Gamma(p)}\frac{1}{\left(M^2-\mathbf{k}^2\right)^{(p-d/2)}}\quad, \tag{B4}$$

where $S_d=2^{1-d}\pi^{-d/2}/\Gamma(d/2)$ is related to the surface of the d-dimensional unit sphere. Due to the Feynman parametrization (B3) of our integrals we are left with a parameter integration

$$\overset{\circ}{I}_\sigma(\mathbf{k},\omega)=\frac{S_d}{2\lambda_\circ}\frac{\Gamma(\epsilon/2)\Gamma(2-\epsilon/2)}{2}\int_0^1 ds\left(m_\circ^2+s\frac{\lambda_\circ k^2-i\omega}{2\lambda_\circ}-s^2\frac{k^2}{4}\right)^{-\epsilon/2}\quad. \tag{B5}$$

The expression for $\overset{\circ}{I}_\pi(\mathbf{k},\omega)$ is obtained by setting $m_\circ=0$ in (B5) and the parameter integral can be performed with the help of the hypergeometric function F (Ref. 32)

$$\overset{\circ}{I}_\pi(\mathbf{k},\omega)=\frac{1}{2\lambda_\circ}\frac{A_d}{\epsilon}\left(\frac{\lambda_\circ k^2-i\omega}{2\lambda_\circ}\right)^{-\epsilon/2}F\left(1-\frac{\epsilon}{2},\frac{\epsilon}{2},2-\frac{\epsilon}{2},\frac{1}{2}\frac{\lambda_\circ k^2}{\lambda_\circ k^2-i\omega}\right)\,, \tag{B6}$$

and $A_d=S_d\Gamma(\epsilon/2)\Gamma(1-\epsilon/2)\epsilon/2$ is an abbreviation.[32] The parameter integral of (B5) can be evaluated numerically if necessary, in case of $\mathbf{k}=0$ it can be done analytically

$$\overset{\circ}{I}_\sigma(\mathbf{k}=0,\omega)=\frac{1}{2\lambda_\circ}\frac{A_d}{\epsilon}\frac{2\lambda_\circ}{-i\omega}\left[\left(m_\circ^2-\frac{i\omega}{2\lambda_\circ}\right)^{1-\epsilon/2}-\left(m_\circ^2\right)^{1-\epsilon/2}\right]\quad. \tag{B7}$$

APPENDIX C: HIGH-TEMPERATURE PHASE

The treatment of the theory in the high-temperature phase has to observe that there is a nonvanishing shift of the transition temperature[33]

$$r_{\circ c}(u_\circ,d)=u_\circ^{2/\epsilon}\,S(\epsilon)\quad, \tag{C1}$$

where obviously r_{oc} does not have an expansion in integer powers of u_o. In the low-temperature phase, the variable m, related to the expectation value of the order parameter, naturally included that shift. Above T_c, instead of

$$r_o - r_{oc} = a_o \tau \quad \text{with} \quad \tau = \frac{T - T_c}{T} \quad \text{and} \quad a_o > 0 \quad , \tag{C2}$$

the correlation length is an appropriate choice $\xi = \xi(r_o - r_{oc}, u_o, d)$, whose asymptotic temperature dependence is well known, i.e., $\xi = A_\xi \tau^{-\nu}$.

The subsequent treatment of the symmetric theory follows the same route as elaborated in the low-temperature phase. The definition of Z factors is formally identical, however, as long as we are not interested in describing crossover phenomena, these are functions of the coupling constant only. Their explicit form is well known in literature and here we immediately give the result of a two-loop calculation of the renormalized $\mathbf{\Phi}^2$ correlation function

$$2n\,\Pi\big(\mathbf{k}, \omega, \xi, u, \lambda, \mu\big) = A_d \mu^{-\epsilon}\, \frac{n}{\varepsilon} I_\Phi\left(\frac{k^2}{\mu^2}, \frac{\omega}{\lambda\mu^2}, \xi\mu\right)\left[1 - (n+2)\frac{u}{6\varepsilon} I_\Phi\left(\frac{k^2}{\mu^2}, \frac{\omega}{\lambda\mu^2}, \xi\mu\right)\right] \tag{C3}$$

with the parameter integral of the order parameter bubble

$$I_\Phi\left(\frac{k^2}{\mu^2}, \frac{\omega}{\lambda\mu^2}, \xi\mu\right) = (1 - \varepsilon/2)\int_0^1 ds \left[(\xi\mu)^{-2} + \frac{\lambda k^2 - i\omega}{2\lambda\mu^2} s - \frac{k^2}{4\mu^2} s^2\right]^{-\varepsilon/2} - 1 \quad . \tag{C4}$$

Next we turn to the renormalization-group equation for the $\mathbf{\Phi}^2$ correlation function, whose solution reads

$$\begin{aligned} \frac{2n}{A_d}\hat{\Pi}\big(\frac{\mathbf{k}}{\mu}, \frac{\omega}{\lambda\mu^2}, \xi\mu, u\big) \;=\; & \exp\left[\int_1^l \Big(-2\zeta_{\Phi^2}\big[u(l')\big] - \varepsilon\Big)\frac{dl'}{l'}\right] \frac{2n}{A_d}\hat{\Pi}\left(\frac{\mathbf{k}}{\mu(l)}, \frac{\omega}{\lambda(l)\mu^2(l)}, \xi\mu(l), u(l)\right) \\ & - \int_1^l \hat{B}_{\Phi^2}\big[u(l')\big] \exp\left[\int_1^{l'} \Big(-2\zeta_{\Phi^2}\big[u(l'')\big] - \varepsilon\Big)\frac{dl''}{l''}\right]\frac{dl'}{l'} \,, \end{aligned} \tag{C5}$$

with $\mu(l) = \mu l$. In the range of the Heisenberg fixed point, where $u(l) = u_H^*$, the asymptotic flow equations can be easily integrated yielding $\lambda(l) = \lambda l^{z-2}$, and

$$\exp\left[\int_1^l \Big(-2\zeta_{\Phi^2}\big[u(l')\big] - \varepsilon\Big)\frac{dl'}{l'}\right] = l^{-\alpha/\nu} \quad , \tag{C6}$$

with critical exponents α, z and ν.

A matching condition again prevents the right-hand side of the generalized scaling law (C5) from being infrared singular, but now includes the temperature variable as well

$$\left(\frac{\omega}{\lambda(l)\mu^2(l)}\right)^{4/z} + \left(\Big[\xi\mu(l)\Big]^{-2} + \frac{\mathbf{k}^2}{\mu^2(l)}\right)^2 = 1 \,. \tag{C7}$$

Inserting $\lambda(l)$ from above and using the definition of the characteristic frequency $\omega_{\rm ch} = \lambda\mu^2\,(\mu\xi)^{-z}$, inversion of (C7) yields

$$l = (\mu\xi)^{-1} F\big(k\xi, \omega/\omega_{\rm ch}\big) \quad \text{with} \quad F(x,y) = \Big[\big(1 + x^2\big)^2 + y^{4/z}\Big]^{1/4} \quad . \tag{C8}$$

Now we are ready to obtain from Eq. (C5) the scaling law for the renormalized $\mathbf{\Phi}^2$ correlation function

$$\frac{2n}{A_d}\hat{\Pi}\left(\frac{\mathbf{k}}{\mu}, \frac{\omega}{\lambda\mu^2}, \xi\mu, u\right) = -\frac{\nu}{\alpha}\hat{B}^*_{\Phi^2} + (\xi\mu)^{\alpha/\nu}\, P\big(k\xi, \omega/\omega_{\rm ch}\big) \,, \tag{C9}$$

with the scaling function $P(x,y)$ given by

$$P\Big(x,y\Big) = F^{-\alpha/\nu}(x,y)\left[\hat{B}^*_{\Phi^2}\frac{\nu}{\alpha} + \frac{2n}{A_d}\,\hat{\Pi}\left(\frac{x}{F(x,y)}, \frac{y}{F^z(x,y)}, F(x,y), u^*_H\right)\right] . \tag{C10}$$

Inserting the two-loop amplitude function one obtains an explicit expression for the scaling function, which for $\mathbf{k} = 0$ takes the form

$$P(0,y) = \big(1 + y^{4/z}\big)^{-\alpha/(4\nu)}\left[\hat{B}^*_{\Phi^2}\frac{\nu}{\alpha} + \frac{n}{\varepsilon} f(y)\Big(1 - \frac{n+2}{6\varepsilon} u^*_H f(y)\Big)\right] \quad , \tag{C11}$$

with the auxiliary function

$$f(y)=\frac{2i}{y}\left(1+y^{4/z}\right)^{(z-2+\epsilon)/4}\left[\left(1-\frac{iy}{2}(1+y^{4/z})^{(2-z)/4}\right)^{1-\epsilon/2}-1\right]-1 \quad . \tag{C12}$$

---

*Present address: SIEMENS AG, Mobile Radio Networks, ÖN MN VT 23, Hofmannstrasse 51, 81359 München, Germany.

[1]R.A. Cowley and A.D. Bruce, J. Phys. C **11**, 3577 (1978).
[2]A.D. Bruce and R.A. Cowley, J. Phys. C **11**, 3609 (1978).
[3]G.F. Mazenko, Phys. Rev. B **14**, 3933 (1976).
[4]H.Z. Cummins, Phys. Rep. **185**, 211 (1990).
[5]H. Poulet and R.M. Pick, J. Phys. C **14**, 2675 (1987).
[6]V.V. Lemanov, S.K. Esayan, and A. Karaev, Fiz. Tverd. Tela (Leningrad) **28**, 1683 (1986) [Sov. Phys. Solid State **28**, 931 (1986)].
[7]I. Hatta, M. Hanami, and K. Hamano, J. Phys. Soc. Jpn. **48**, 160 (1980).
[8]L.D. Landau and I.M. Khalatnikov, Dok. Akad. Nauk SSR **96**, 496 (1954).
[9]R. Zeyher, Ferroelectrics **66**, 217 (1986).
[10]S. Hirotsu, K. Toyota, and K. Hamano, Ferroelectrics **36**, 319 (1981).
[11]G. Li, N. Tao, L. Van Hong, H.Z. Cummins, C. Dreyfus, M. Hebbache, R.M. Pick, and J. Vagner, Phys. Rev. B **42**, 4406 (1990).
[12]R. Dengler and F. Schwabl, Z. Phys. B **69**, 327 (1987).
[13]I.D. Lawrie, J. Phys. A **14**, 2489 (1981); J. Phys. A **18**, 1141 (1985).
[14]U.C. Täuber and F. Schwabl, Phys. Rev. B **46**, 3337 (1992).
[15]A.M. Schorgg and F. Schwabl, Phys. Lett. A **168**, 437 (1992).
[16]A.M. Schorgg and F. Schwabl, Phys. Rev. B **46**, 8828 (1992).
[17]Y. Ishibashi, in *Incommensurate Phases in Dielectrics—2. Materials*, edited by R. Blinc and A.P. Levanyuk (North-Holland, Amsterdam, 1986).
[18]F. Schwabl, Ferroelectrics **78**, 215 (1988).
[19]A.P. Mayer and R.A. Cowley, J. Phys. C **19**, 6131 (1986).
[20]R. Zeyher and W. Finger, Phys. Rev. Lett. **49**, 1833 (1982).
[21]P.C. Hohenberg and B.I. Halperin, Rev. Mod. Phys. **49**, 435 (1977).
[22]B. Drossel and F. Schwabl, Z. Phys. B **91**, 93 (1993).
[23]T. Nattermann, J. Phys. A **10**, 1757 (1977); M.A. de Moura, T.C. Lubensky, Y. Ymry, and A. Aharony, Phys. Rev. B **13**, 2176 (1976).
[24]R.A. Ferrell and J.K. Bhattacharjee, Phys. Rev. B **35**, 4662 (1987).
[25]H.K. Janssen, Z. Phys. B **23**, 377 (1976).
[26]R. Bausch, H.K. Janssen, and H. Wagner, Z. Phys. B **24**, 113 (1976).
[27]P.C. Martin, E.D. Siggia, and H.A. Rose, Phys. Rev. A **8**, 423 (1973).
[28]G. t'Hooft and M. Veltman, Nucl. Phys. **B44**, 189 (1972).
[29]I.D. Lawrie, J. Phys. A **9**, 961 (1976).
[30]D.J. Amit and Y.Y. Goldschmidt, Ann. Phys. **114**, 356 (1978).
[31]E. Frey and F. Schwabl, J. Phys. (Paris) Colloq. **48**, C8-1569 (1988); Phys. Rev. B **42**, 8261 (1990); **43**, 833 (1991).
[32]M. Abramowitz and I.A. Stegun, *Handbook of Mathematical Functions* (Dover, New York, 1962).
[33]R. Schloms and V. Dohm, Nucl. Phys. **B328**, 639 (1989).
[34]M.N. Barber, Phys. Rep. **29**, 1 (1977).
[35]R.A. Ferrell and J.K. Bhattacharjee, Phys. Rev. B **23**, 2434 (1981).
[36]H. Mashiyama, S. Tanisaki, and K. Hamano, J. Phys. Soc. Jpn. **50**, 2139 (1981).
[37]S. Hirotsu, K. Toyota, and K. Hamano, J. Phys. Soc. Jpn. **46**, 1389 (1979).
[38]V.V. Lemanov and S.K. Esayan, Ferroelectrics **73**, 125 (1987).
[39]R. Blinc, in *Incommensurate Phases in Dielectrics—1. Fundamentals*, edited by R. Blinc and A.P. Levanyuk (North-Holland, Amsterdam, 1986).
[40]R. Walisch, J.M. Perez-Mato, and J. Petersson, Phys. Rev. B **40**, 10 747 (1989).
[41]Z.Y. Chen, Phys. Rev. B **41**, 9516 (1990).
[42]Z. Hu, C.W. Garland, and S. Hirotsu, Phys. Rev. B **42**, 8305 (1990).
[43]A.M. Schorgg, Ph.D. thesis, Technische Universität München, 1993.